Table 1
Particle characteristics of TiO_2.

	Crystal form	Size
A-1	Anatase	<50 μm
A-2	Anatase	<25 nm
A-3	Anatase	10 nm
R-1	Rutile	<5 μm
R-2	Rutile	30–40 nm
R-3	Rutile	10 nm × 40 nm (spicula)

multimolecular complex termed the inflammasome [14]. The NACHT domain-, leucine-rich repeat-, and pyrin domain (PYD)-containing protein 3 (NALP3) inflammasome, composed of the cytoplasmic receptor NALP3, the adaptor apoptosis-associated speck-like protein containing a CARD domain (ASC), and caspase-1, is implicated in the production of mature IL-1β in response to diverse stimuli [15]. Although the mechanisms of NALP3 activation remain unclear, two separate groups have recently clarified the mediator of NALP3 activation: Cassel et al. demonstrated that phagocytosis of crystalline silica by macrophages induces reactive oxygen species (ROS) production, which contributes to NALP3 activation [16], and Hornung et al. showed that it induces lysosomal destabilization and subsequent release of cathepsin B into the cytoplasm, leading to NALP3 activation [17]. However, it is unclear whether the TiO_2-induced IL-1β production is similarly dependent on NALP3 activation, and it is unknown whether different forms of TiO_2 induce IL-1β production in common or distinct pathways.

Here, we examined the associations between characteristics of forms of TiO_2 and IL-1β production. In addition, we investigated the IL-1β production mechanisms induced by various forms of TiO_2 on macrophage-like THP-1 cells for the creation of novel safe forms of TiO_2.

Materials and methods

Materials and reagents. We used various forms of TiO_2 with two types of crystal structure, different diameters, and different shapes: anatase (A-1 to A-3) and rutile TiO_2 (R-1 to R-3) (Table 1). A-1 to A-3, R-1, and R-2 are spherical, while R-3 is spicular. A-1, A-2, R-1, and R-3 were purchased from Sigma (St. Louis, MO, USA), and A-3 and R-2 were purchased from NanoAmor (Los Alamos, NM, USA). Phorbol 12-myristate 13-acetate (PMA), cytochalasin D, methyl-β-cyclodextrin (MBCD), butylated hydroxyanisole (BHA), diphenyleneiodonium chloride (DPI), and lipopolysaccharide (LPS) were purchased from Sigma. Bafilomycin A_1 was purchased from Biomol (Plymouth Meeting, PA, USA). CA-074-methyl ester (CA-074-Me) and zYVAD-fmk were purchased from Merck Calbiochem (Darmstadt, Germany).

Cells. THP-1 cells (human acute monocytic leukemia cell line) were obtained from the American Type Culture Collection (Manassas, VA, USA) and cultured in RPMI-1640 medium (Wako Pure Chemical Industries, Osaka, Japan) supplemented with 10% fetal bovine serum, 2 mM L-glutamine, and antibiotics at 37 °C in a humid atmosphere with 5% CO_2.

Cytokine production induced by TiO_2. THP-1 cells (1.5×10^4 cells/well) were seeded in 96-well plates (Nunc, Rochester, NY, USA). Differentiation of monocytic THP-1 cells into macrophages was induced by incubation with PMA (0.5 μM) for 24 h at 37 °C. Differentiated cells were then stimulated with 20, 100, or 500 μg/mL TiO_2 for 24 h in the presence or absence of LPS, a widely known activator of THP-1 cells. The levels of IL-1β and tumor necrosis factor α (TNFα) in culture supernatants were then assessed by a commercial enzyme-linked immunosorbent assay (ELISA) kit (BD Pharmingen, San Diego, CA, USA) according to the manufacturer's instructions. For assay of inhibitors, PMA-primed THP-1 cells were washed and pre-incubated with cytochalasin D (1 or 5 μM), MBCD (10 μM), zYVAD-fmk (5 or 10 μM), bafilomycin A_1 (50 or 250 nM), CA-074-Me (5 or 10 μM), BHA (20 or 100 μM), or DPI (10 μM) for 30 min. Then cells were stimulated with 500 μg/mL TiO_2 or 3 mM ATP (a well-known IL-1β inducer) for 6 h in the presence of each inhibitor.

Phagocytosis of TiO_2 on PMA-primed THP-1 cells. THP-1 cells (1.5×10^4 cells/well) were seeded in 96-well plates and primed with PMA (0.5 μM) for 24 h at 37 °C. Differentiated cells were then

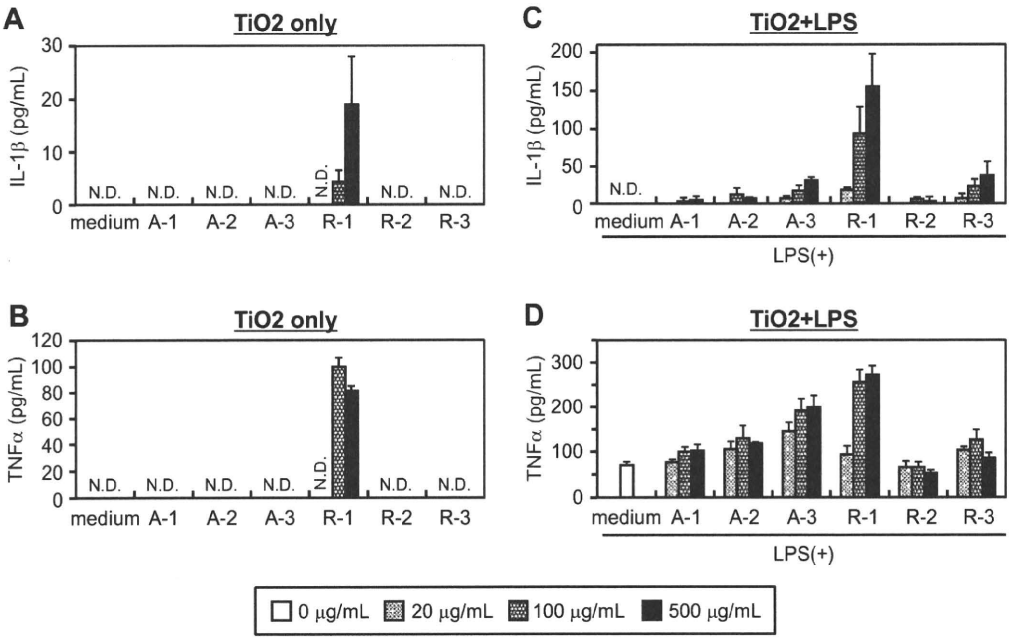

Fig. 1. Association between the characteristics of TiO_2 and cytokine production by THP-1 monocytes. THP-1 monocyte cells were stimulated with 20, 100, or 500 μg/mL of various forms of TiO_2 in the absence (A, B) or presence (C, D) of LPS, and the IL-1β (A, C) or TNFα (B, D) concentrations in the supernatants were evaluated by ELISA. N.D., not detected. Data represent mean ± SD ($n = 4$).

treated with 20 μg/mL TiO_2 for 24 h, and then photographed through a fluorescence microscope (BZ-8000; Keyence Corporation, Osaka, Japan).

Statistical analysis. All results are presented as means ± standard deviation (SD). Differences were compared by Scheffé's method after analysis of variance (ANOVA).

Results and discussion

IL-1β production levels depend on the characteristics of TiO_2

To compare the inflammatory responses, we systematically analyzed the association between characteristics of TiO_2 and levels of IL-1β and TNFα production. We incubated monocytic THP-1 cells with each form of TiO_2 in the absence (Fig. 1A and B) or presence (Fig. 1C and D) of LPS. In the absence of LPS, the larger R-1 induced higher levels of IL-1β and TNFα production than the other forms of TiO_2 (Fig. 1A and B). In the presence of LPS, A-3, and R-3 also induced higher levels of IL-1β production (Fig. 1C). Next we tested PMA-primed macrophage-like THP-1 (THP-1/PMA) cells. Each form of TiO_2 was ingested by THP-1/PMA cells, suggesting that THP-1/PMA cells recognized the TiO_2 as foreign (Fig. 2A). At all concentrations, rutile (especially R-1 and R-3) induced higher IL-1β production than anatase (Fig. 2B). Interestingly, the smallest anatase, A-3, induced higher IL-1β production than the larger A-1 and A-2, whereas the largest rutile, R-1, induced higher IL-1β production than the smaller R-2 and R-3 (Fig. 2B). In addition, spicular R-3 induced higher IL-1β production than the similarly sized and structurally identical but spherical R-2 at the lower concentrations (20 and 100 μg/mL). These results indicate that it is necessary to compare multiple characteristics, including particle size, crystal structure, physical attributes, and surface properties, of TiO_2 to elucidate its biological effects. From these observations, we decided to use A-3, R-1, R-2, and R-3 in further examinations.

Phagocytosis of TiO_2 is an upstream signal in the induction of IL-1β production

Phagocytosis is a key event in initiating macrophage-derived inflammatory responses, and under certain conditions requires lipid raft domains [18,19]. To investigate the association between phagocytosis and TiO_2-induced IL-1β production, we stimulated THP-1/PMA cells with TiO_2 or ATP (control) in the presence of cytochalasin D, a well-characterized inhibitor of phagocytosis that impairs actin-filament assembly. ATP induces IL-1β without cellular internalization and lipid raft formation [20]. Cytochalasin D dramatically abrogated IL-1β production induced by TiO_2, whereas the response to ATP was relatively unaffected (Fig. 3A). Similar results were obtained with MBCD, an inhibitor of lipid raft formation (Fig. 3B). These results indicate that lipid rafts and actin-filament-dependent phagocytosis might be early signals in TiO_2-induced IL-1β production.

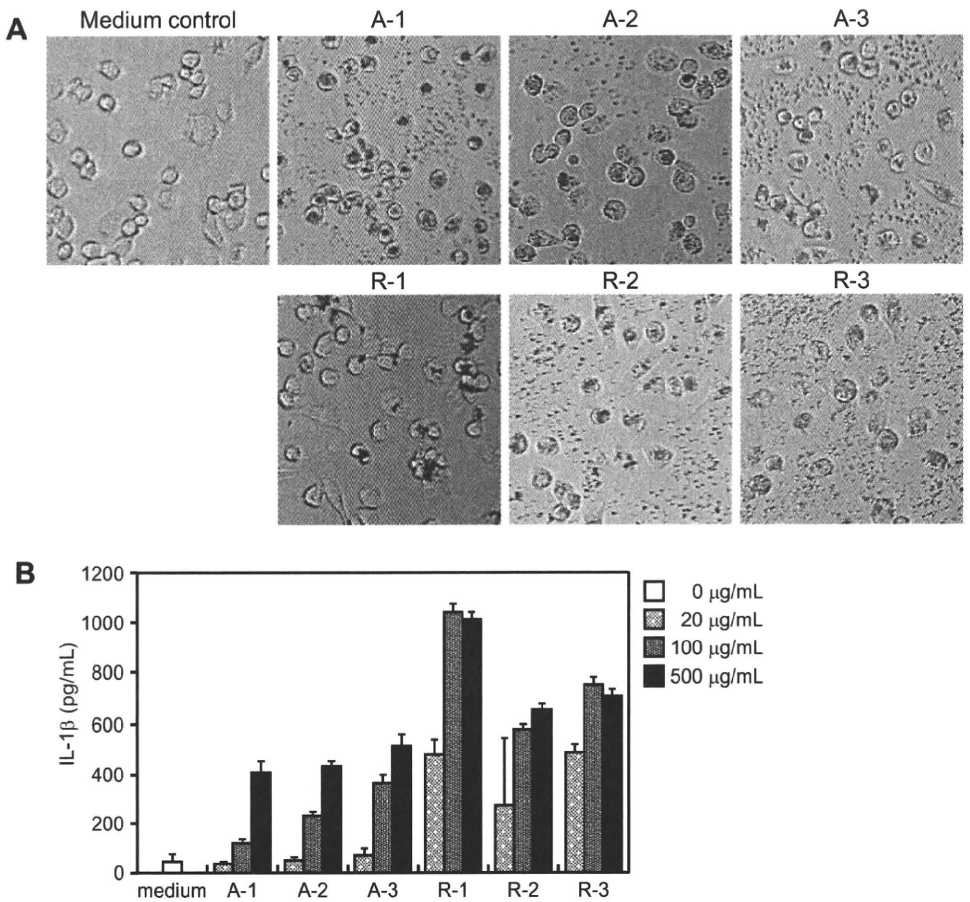

Fig. 2. Association between the characteristics of TiO_2 and cytokine production by differentiated macrophage-like THP-1/PMA cells. (A) THP-1/PMA cells were stimulated with 20 μg/mL of various forms of TiO_2 for 24 h and photographed through a fluorescence microscope. (B) THP-1/PMA cells were stimulated with 20, 100, or 500 μg/mL of various forms of TiO_2 for 6 h, and the IL-1β concentration in the supernatant was evaluated by ELISA. Data represent mean ± SD ($n = 4$; $^{**}P < 0.01$ vs. control).

TiO_2-induced IL-1β production by THP-1/PMA cells depended on caspase-1, ROS, and cathepsin B

Next, we examined how TiO_2 induces IL-1β production. IL-1β is produced from the inactive precursor pro-IL-1β in the cytosol. After cellular activation by a variety of stimuli, the maturation of pro-IL-1β into the mature IL-1β is controlled by caspase-1 [14,21]. To confirm the activation by caspase-1, we treated cells with a caspase-1-specific inhibitor, zYVAD-fmk [22]. zYVAD-fmk completely blocked both ATP- and TiO_2-induced IL-1β production (Fig. 4A), suggesting that the release of IL-1β by TiO_2 is mediated by activated caspase-1.

After assembly of the inflammasome, which activates pro-caspase-1, caspase-1 controls IL-1β maturation. However, how the inflammasome is activated is not well understood. Recently, Hornung et al. reported that crystalline silica induces lysosomal enlargement and loss of lysosomal integrity, leading to the release of the lysosomal contents into the cytoplasm. Furthermore, the release of specific proteases such as cathepsin B seems to be causally related to inflammasome activation [17]. To investigate

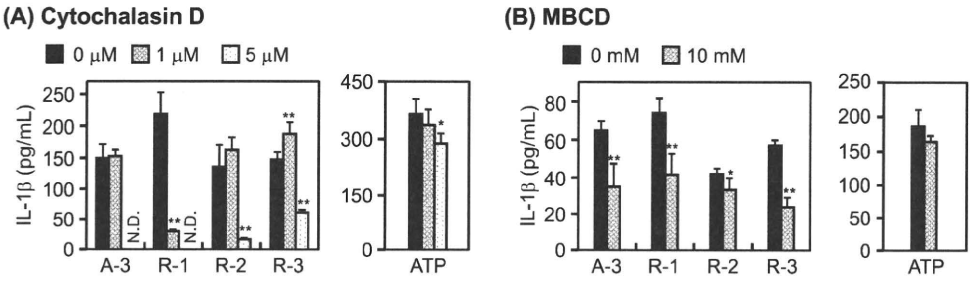

Fig. 3. TiO_2-induced IL-1β production in THP-1/PMA cells is mediated by phagocytosis and lipid rafts. (A, B) IL-1β production levels of THP-1/PMA cells stimulated with 500 μg/mL TiO_2 or 5 mM ATP for 6 h in the presence or absence of (A) cytochalasin D or (B) MBCD at indicated concentrations. IL-1β levels in the culture media were analyzed by ELISA. N.D., not detected. Data represent mean ± SD ($n = 4$; $^{*}P < 0.05$ and $^{**}P < 0.01$ vs. inhibitor [−]).

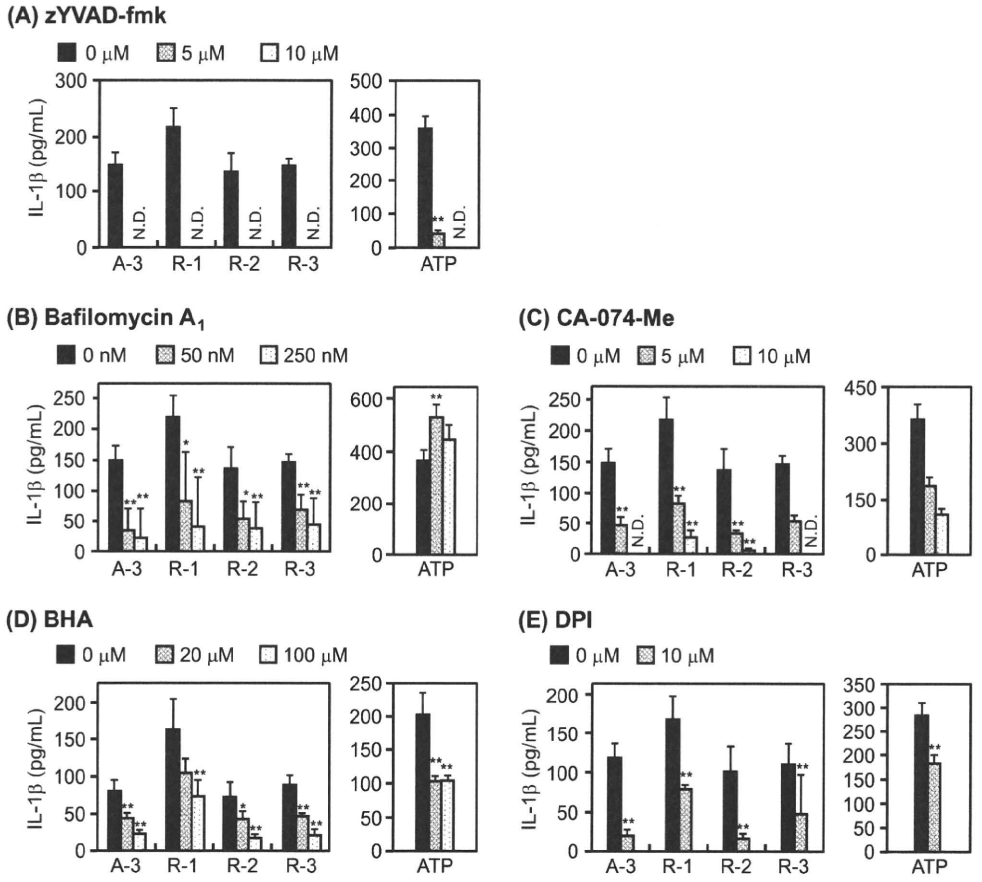

Fig. 4. TiO_2-induced IL-1β production in THP-1/PMA cells is mediated by caspase-1, ROS, and cathepsin B. (A–E) IL-1β production levels of THP-1/PMA cells stimulated with 500 μg/mL TiO_2 or 5 mM ATP for 6 h in the presence or absence of (A) zYVAD-fmk, (B) bafilomycin A_1, (C) CA-074-Me, (D) BHA, or (E) DPI at indicated concentrations. IL-1β levels in the culture media were analyzed by ELISA. N.D., not detected. Data represent mean ± SD ($n = 4$; $^{*}P < 0.05$ and $^{**}P < 0.01$ vs. inhibitor [−]).

whether cathepsin B mediates TiO_2-induced IL-1β production, we stimulated THP-1/PMA cells with TiO_2 in the presence of a specific inhibitor of the vacuolar H^+-ATPase (bafilomycin A_1) or a membrane-permeable cathepsin B-specific inhibitor (CA-074-Me). Bafilomycin A_1 suppresses the pH decrease in endo-lysosomes; the pH decrease is important for cathepsin B to exert its activity. Both inhibitors almost completely suppressed the IL-1β production induced by TiO_2 independent of the characteristics of TiO_2 (Fig. 4B and C), suggesting that the active cathepsin B is one of the most important common activators of the inflammasome upon TiO_2 stimulation.

It is well known that the stimulation of macrophages with TiO_2 induces ROS production. The inflammasome activator ATP can induce the production of ROS, which are important for caspase-1 activation, suggesting that ROS signaling occurs upstream of inflammasome [16,23,24]. To examine whether ROS are involved in the TiO_2-induced IL-1β production, we stimulated THP-1/PMA cells with TiO_2 in the presence of a broad ROS scavenger, BHA. BHA significantly inhibited the TiO_2-induced IL-1β production (Fig. 4D). We obtained similar results in cells treated with DPI, a specific inhibitor of NADPH-oxidase, an important enzyme in the production of ROS (Fig. 4E) [25]. These results indicate that both cathepsin B and ROS play important roles in TiO_2-induced IL-1β production independent of particle characteristics. We speculate that caspase-1, cathepsin B, and ROS are mutually linked in a single pathway for the TiO_2-induced IL-1β-producing cascade. However, it is unclear how the ROS and cathepsin B interact with each other. Recently, Blomgran et al. showed that ROS production in microbes induces lysosomal rupture, allowing cathepsin B to leak into the cytoplasm [26]. Therefore, we speculate that TiO_2-induced ROS induce lysosomal rupture and subsequent inflammasome/caspase-1 activation. On the other hand, some reports show that after phagocytosis of crystalline silica, the reactive particle surface may interact with the phagolysosomal membranes, leading to lysosomal rupture. This suggests that the surface properties of TiO_2 influence the permeability of the lysosomal membrane [27–29]. We are now examining the association between particle characteristics of TiO_2 and lysosomal responses.

Our results confirm that characteristics of TiO_2 change the activity of posttranscriptional processing of IL-1β mediated by caspase-1. However, for several inflammatory cytokines, including IL-1β, both transcription and posttranslational processing are important for the secretion of their mature forms [17,23,30]. Nuclear factor-κB (NFκB) is a well-known transcription factor that regulates the transcription of various cytokines, including IL-1β and TNFα. Therefore, it is important to investigate the association between characteristics of TiO_2 and NFκB activity for the development of safe forms of TiO_2.

The development of safe and effective nanomaterials is important for technology advancement and for healthy lives. For the creation of such materials, we need more information about the relationship between particle characteristics and biological effects. It has become evident that the surface properties of particles are also very important factors in biological effects [7,9,31]. Therefore, we are now trying to develop a novel method for designing TiO_2 particles, including surface properties, crystal structure, size, and shape, to enable the creation of safe and effective novel materials.

Conclusion

The inflammatory effect of TiO_2 depended dramatically on the particle characteristics. TiO_2-induced IL-1β production was mediated by ROS and cathepsin B independent of the particle characteristics. These results provide important basic information for the development of safe forms of TiO_2.

Conflict of interest

The authors declare that they have no conflicts of interest.

Acknowledgments

This study was supported in part by grants from the Ministry of Education, Culture, Sports, Science and Technology of Japan, and the Ministry of Health, Labor and Welfare in Japan.

References

[1] C.L. Tran, D. Buchanan, R.T. Cullen, et al., Inhalation of poorly soluble particles: II. Influence of particle surface area on inflammation and clearance, Inhal. Toxicol. 12 (2000) 1113–1126.
[2] P.M. Hext, J.A. Tomenson, P. Thompson, Titanium dioxide: inhalation toxicology and epidemiology, Ann. Occup. Hyg. 49 (2005) 461–472.
[3] K.E. Driscoll, J.K. Maurer, Cytokine and growth factor release by alveolar macrophages: potential biomarkers of pulmonary toxicity, Toxicol. Pathol. 19 (1991) 398–405.
[4] E. Bermudez, J.B. Mangum, B.A. Wong, et al., Pulmonary responses of mice, rats, and hamsters to subchronic inhalation of ultrafine titanium dioxide particles, Toxicol. Sci. 77 (2004) 347–357.
[5] E.J. Park, J. Yi, K.H. Chung, et al., Oxidative stress and apoptosis induced by titanium dioxide nanoparticles in cultured BEAS-2B cells, Toxicol. Lett. 180 (2008) 222–229.
[6] J. Wang, Y. Liu, F. Jiao, et al., Time-dependent translocation and potential impairment on central nervous system by intranasally instilled TiO(2) nanoparticles, Toxicology 254 (2008) 82–90.
[7] D. Napierska, L.C. Thomassen, V. Rabolli, et al., Size-dependent cytotoxicity of monodisperse silica nanoparticles in human endothelial cells, Small 5 (2009) 846–853.
[8] E.J. Park, J. Yoon, K. Choi, et al., Induction of chronic inflammation in mice treated with titanium dioxide nanoparticles by intratracheal instillation, Toxicology 260 (2009) 37–46.
[9] K.M. Waters, L.M. Masiello, R.C. Zangar, et al., Macrophage responses to silica nanoparticles are highly conserved across particle sizes, Toxicol. Sci. 107 (2009) 553–569.
[10] B.B. Aggarwal, P. Gehlot, Inflammation and cancer: how friendly is the relationship for cancer patients?, Curr Opin. Pharmacol. 9 (2009) 351–369.
[11] L. Franchi, T. Eigenbrod, R. Munoz-Planillo, et al., The inflammasome: a caspase-1-activation platform that regulates immune responses and disease pathogenesis, Nat. Immunol. 10 (2009) 241–247.
[12] P.F. Piguet, C. Vesin, G.E. Grau, et al., Interleukin 1 receptor antagonist (IL-1ra) prevents or cures pulmonary fibrosis elicited in mice by bleomycin or silica, Cytokine 5 (1993) 57–61.
[13] P.N. Hawkins, H.J. Lachmann, M.F. McDermott, Interleukin-1-receptor antagonist in the Muckle–Wells syndrome, N. Engl. J. Med. 348 (2003) 2583–2584.
[14] L. Agostini, F. Martinon, K. Burns, et al., NALP3 forms an IL-1beta-processing inflammasome with increased activity in Muckle–Wells autoinflammatory disorder, Immunity 20 (2004) 319–325.
[15] A. Halle, V. Hornung, G.C. Petzold, et al., The NALP3 inflammasome is involved in the innate immune response to amyloid-beta, Nat. Immunol. 9 (2008) 857–865.
[16] S.L. Cassel, S.C. Eisenbarth, S.S. Iyer, et al., The Nalp3 inflammasome is essential for the development of silicosis, Proc. Natl. Acad. Sci. USA 105 (2008) 9035–9040.
[17] V. Hornung, F. Bauernfeind, A. Halle, et al., Silica crystals and aluminum salts activate the NALP3 inflammasome through phagosomal destabilization, Nat. Immunol. 9 (2008) 847–856.
[18] M. Kirkham, R.G. Parton, Clathrin-independent endocytosis: new insights into caveolae and non-caveolar lipid raft carriers, Biochim. Biophys. Acta 1745 (2005) 273–286.
[19] M.F. Hanzal-Bayer, J.F. Hancock, Lipid rafts and membrane traffic, FEBS Lett. 581 (2007) 2098–2104.
[20] C.M. Cruz, A. Rinna, H.J. Forman, et al., ATP activates a reactive oxygen species-dependent oxidative stress response and secretion of proinflammatory cytokines in macrophages, J. Biol. Chem. 282 (2007) 2871–2879.
[21] F. Martinon, V. Petrilli, A. Mayor, et al., Gout-associated uric acid crystals activate the NALP3 inflammasome, Nature 440 (2006) 237–241.
[22] S. Mariathasan, D.S. Weiss, K. Newton, et al., Cryopyrin activates the inflammasome in response to toxins and ATP, Nature 440 (2006) 228–232.
[23] C. Dostert, V. Petrilli, R. Van Bruggen, et al., Innate immune activation through Nalp3 inflammasome sensing of asbestos and silica, Science 320 (2008) 674–677.
[24] M.E. Carlotti, E. Ugazio, S. Sapino, et al., Role of particle coating in controlling skin damage photoinduced by titania nanoparticles, Free Radic. Res. 43 (2009) 312–322.
[25] F. Morel, J. Doussiere, P.V. Vignais, The superoxide-generating oxidase of phagocytic cells. Physiological, molecular and pathological aspects, Eur. J. Biochem. 201 (1991) 523–546.

[26] R. Blomgran, L. Zheng, O. Stendahl, Cathepsin-cleaved Bid promotes apoptosis in human neutrophils via oxidative stress-induced lysosomal membrane permeabilization, J. Leukoc. Biol. 81 (2007) 1213–1223.
[27] A.C. Allison, J.S. Harington, M. Birbeck, An examination of the cytotoxic effects of silica on macrophages, J. Exp. Med. 124 (1966) 141–154.
[28] S. Nadler, S. Goldfischer, The intracellular release of lysosomal contents in macrophages that have ingested silica, J. Histochem. Cytochem. 18 (1970) 368–371.
[29] G. Erdogdu, V. Hasirci, An overview of the role of mineral solubility in silicosis and asbestosis, Environ. Res. 78 (1998) 38–42.
[30] S.D. Ha, A. Martins, K. Khazaie, et al., Cathepsin B is involved in the trafficking of TNF-alpha-containing vesicles to the plasma membrane in macrophages, J. Immunol. 181 (2008) 690–697.
[31] X. He, H. Nie, K. Wang, et al., In vivo study of biodistribution and urinary excretion of surface-modified silica nanoparticles, Anal. Chem. 80 (2008) 9597–9603.

Biomaterials 31 (2010) 6833–6842

Contents lists available at ScienceDirect

Biomaterials

journal homepage: www.elsevier.com/locate/biomaterials

The effect of surface modification of amorphous silica particles on NLRP3 inflammasome mediated IL-1β production, ROS production and endosomal rupture

Tomohiro Morishige [a,1], Yasuo Yoshioka [a,b,c,*,1], Hiroshi Inakura [a], Aya Tanabe [a], Xinglei Yao [a], Shogo Narimatsu [a], Youko Monobe [d], Takayoshi Imazawa [d], Shin-ichi Tsunoda [b,c], Yasuo Tsutsumi [b,c,e], Yohei Mukai [a], Naoki Okada [a], Shinsaku Nakagawa [a,b,**]

[a] Laboratory of Biotechnology and Therapeutics, Graduate School of Pharmaceutical Sciences, Osaka University, 1–6 Yamadaoka, Suita, Osaka 565–0871, Japan
[b] The Center for Advanced Medical Engineering and Informatics, Osaka University, 1–6 Yamadaoka, Suita, Osaka 565–0871, Japan
[c] Laboratory of Pharmaceutical Proteomics, National Institute of Biomedical Innovation, 7–6–8 Saito-Asagi, Ibaraki, Osaka 567–0085, Japan
[d] Laboratory of Common Apparatus, Division of Biomedical Research, National Institute of Biomedical Innovation, 7–6–8 Saito-Asagi, Ibaraki, Osaka 567–0085, Japan
[e] Laboratory of Toxicology and Safety Science, Graduate School of Pharmaceutical Sciences, Osaka University, 1–6 Yamadaoka, Suita, Osaka 565–0871, Japan

ARTICLE INFO

Article history:
Received 23 April 2010
Accepted 18 May 2010
Available online 18 June 2010

Keywords:
Cytokine
Inflammation
Interleukin
Macrophage
Nanoparticle
Silica

ABSTRACT

Although amorphous silica particles (SPs) are widely used in cosmetics, foods and medicinal products, it has gradually become evident that SPs can induce substantial inflammation accompanied by interleukin-1β (IL-1β) production. Here, to develop safe forms of SPs, we examined the mechanisms of SP-induced inflammation and the relationship between particle characteristics and biological responses. We compared IL-1β production levels in THP-1 human macrophage like cells in response to unmodified SP of various diameters (30- to 1000-nm) and demonstrated that unmodified microsized 1000-nm SP (mSP1000) induced higher levels of IL-1β production than did smaller unmodified SPs. Furthermore, we found that unmodified mSP1000–induced IL-1β production was depended on the sequence of reactive oxygen species (ROS) production, endosomal rupture, and subsequent activation of pro-inflammatory complex NLRP3 inflammasome. In addition, we compared IL-1β production levels in THP-1 cells treated with mSP1000s modified with a functional group (−COOH, $-NH_2$, $-SO_3H$, −CHO). Although unmodified and surface-modified mSP1000s were taken up with similar frequencies equally into the THP-1 cells, surface modification of mSP1000 dramatically suppressed IL-1β production by reducing ROS production. Our results reveal a part of NLRP3 activation pathway and provide basic information that should help to create safe and effective forms of SPs.

1. Introduction

Amorphous (noncrystalline) silica particles (SPs) possess extraordinary advantages, including straightforward synthesis, relatively low cost, easy separation, and easy surface modification. In addition, SPs are usually considered to have low toxicity, in contrast to crystalline silica, which can cause silicosis and some forms of lung cancer [1,2]. Therefore, SPs have been used for many applications, including in cosmetics, foods, medical diagnosis, cancer therapy, and drug delivery [3–7].

However, the increasing use of SPs has raised public concern about their safety. In fact, current studies have found that SPs induce substantial lung inflammation accompanied by the expression of inflammatory cytokines, including interleukin-1β (IL-1β) [8–10]. Inflammation has been suggested as the key factor in the development of chronic obstructive pulmonary disease (COPD), fibrosis, and carcinogenesis [11–13]. There is therefore an urgent need to investigate the biological inflammatory effects of SPs and ensure their safe use. In addition, it has recently become evident that particle characteristics, including particle size and surface properties, are important factors in pathologic alterations and cellular responses [14–16]. Therefore, for the further development

* Corresponding author at: The Center for Advanced Medical Engineering and Informatics, Osaka University, 1-6 Yamadaoka, Suita, Osaka 565-0871, Japan. Tel./fax: +81 6 6879 8177.
** Corresponding author at: Laboratory of Biotechnology and Therapeutics, Graduate School of Pharmaceutical Sciences, Osaka University, 1-6 Yamadaoka, Suita, Osaka 565-0871, Japan. Tel.: +81 6 6879 8175; fax: +81 6 6879 8179.
E-mail addresses: yasuo@phs.osaka-u.ac.jp (Y. Yoshioka), nakagawa@phs.osaka-u.ac.jp (S. Nakagawa).
[1] Each author contributed equally to the work.

0142-9612/$ – see front matter © 2010 Elsevier Ltd. All rights reserved.
doi:10.1016/j.biomaterials.2010.05.036

of safe SPs, investigation of the mechanisms of SP-induced inflammation and development of a methodology to decrease their inflammatory effects on the basis of evidence of the correlation between particle characteristics and biological effects are very important.

IL-1β is involved in initiation of the inflammatory process and thus contributes to acute and chronic inflammatory diseases. In fact, Cassel et al. reported the possibility that IL-1β induced by inhalation of crystalline silica and asbestos is essential for the development of silicosis and asbestosis, and thus it is needed to investigate whether SPs induce IL-1β production [17–19]. Among the most important sources of IL-1β against inhaled foreign particles are macrophages, which are widely known as the first line of defense [20]. Recently, several studies have shown that the action of macrophage-derived IL-1β is mediated by the activation of a multi-protein complex, called nucleotide-binding oligomerization domain–leucine-rich repeats containing pyrin domain 3 (NLRP3) inflammasome [20]. Production of the cytoplasmic NLRP3 is associated with fever syndromes characterized by spontaneous inflammation [21]. After being activated, NLRP3 interacts with the adaptor molecule apoptosis-associated speck-like protein containing a caspase recruitment domain (ASC) to form a pro-inflammatory complex, NLRP3 inflammasome, which is the principal caspase-1 activator [17,22,23]. Active caspase-1 catalyzes cleavage of the pro-cytokine IL-1β, which is secreted and biologically active only in processed form [23]. Thus, NLRP3 inflammasome is now gaining attention for its role in the initial inflammation generated in response to a number of diverse stimuli [22,24–26]. However, it is unclear whether SPs induce NLRP3 inflammasome activation. Moreover, the mechanisms of activation of NLRP3 inflammasome are poorly understood.

With the aim of developing safe forms of SPs, we evaluated the correlation between inflammatory effect and particle characteristics of SPs of various sizes or with various surface modification groups. Furthermore, we investigated the mechanisms of IL-1β production induced by SPs, concentrating on NLRP3 inflammasome.

2. Materials and methods

2.1. Materials and reagents

Unmodified SPs of diameters between 30 and 1000 nm [nanosized (n)SP30, nSP70, and nSP300, and microsized (m)SP1000], various surface-modified 1000-nm SPs (mSP1000–COOH, $-NH_2$, $-SO_3H$, and $-CHO$) and FITC-conjugated mSP1000s (unmodified, $-COOH$, $-NH_2$, $-SO_3H$, and $-CHO$) were purchased from Micromod Partikeltechnologie (Rostock/Warnemünde, Germany). Phorbol 12-myristate 13-acetate (PMA), cytochalasin D, butylated hydroxyanisole (BHA), and diphenyleneiodonium chloride (DPI) were purchased from Sigma–Aldrich (St. Louis, MO). Bafilomycin A_1 was purchased from Biomol (Plymouth Meeting, PA). CA-074-methyl ester (CA-074-Me), zVAD-fmk, and zYVAD-fmk was purchased from Merck (Darmstadt, Germany).

2.2. Cells and mice

THP-1 (human acute monocytic leukemia cell line) cells were obtained from the American Type Culture Collection (Manassas, VA) and cultured at 37 °C in RPMI (Wako Pure Chemical Industries, Osaka, Japan) supplemented with 10% FBS, 2 mM L-glutamine, and antibiotics. Female C57BL/6 mice were purchased from Nippon SLC (Shizuoka, Japan) and used at 8 weeks of age. All of the animal experimental procedures were performed in accordance with Osaka University's guidelines for the welfare of animals.

2.3. Characterization of silica particle

Size distribution of each SP was measured using a Zetasizer 3000HS (Worcestershire, UK) after sonication with a particle concentration of 300 μg/mL in H_2O.

2.4. Cytotoxicity assay and enzyme-linked immunosorbent assay (ELISA)

THP-1 cells (1.5×10^4 cells/well) were seeded in 96-well plates (Nunc, Rochester, NY) and were then differentiated into macrophages by incubation with 0.5 μM PMA at 37 °C for 24 h followed by one wash with cell culture medium. After the PMA priming, cells were treated with SPs at 100 μg/mL or 3 mM ATP for 6 or 24 h. Cytotoxicity of the SPs was assessed by the standard methylene blue assay method, as previously described [27]. IL-1β production levels in the culture supernatants were assessed with an ELISA kit (BD Pharmingen, San Diego, CA) in accordance with the manufacturer's instructions. For the inhibitory assay, PMA-primed THP-1 cells were pre-incubated for 30 min with cytochalasin D (5 μM), zYVAD-fmk (10 μM), CA-074-Me (2 μM), bafilomycin A_1 (250 nM), BHA (150 μM), DPI (60 μM), or zVAD-fmk (60 μM). The cells were then treated with SPs at 100 μg/mL or with 3 mM ATP for 6 or 24 h.

2.5. In vivo inflammatory effect

C57BL/6 mice were intraperitoneally injected with 1 mg mSP1000s in 200 μL PBS. Six hours after the treatment, the mice were sacrificed and all of the peritoneal cavity lavage fluid (PCLF) was collected in 4 mL PBS. The total number of live cells in the PCLF was determined with a NucleoCounter (Chemometec A/S, Allerød, Denmark).

2.6. Laser scanning confocal microscopy analysis

THP-1 cells (1×10^5 cells/well) were primed with PMA on a Lab-Tek II Chambered Coverglass (Nunc) and incubated for 6 h with 500 μg/mL 10-kDa dextran conjugated with Alexa Fluor 594 (Invitrogen, Carlsbad, CA) and 100 μg/mL mSP1000. The cells were washed and then fixed with 4% paraformaldehyde, and mounted with Prolong Gold Antifade Reagent with DAPI (Invitrogen) for nuclear staining. Fluorescence was observed under a laser scanning confocal microscope (TCS SP2 AOBS; Leica Microsystems, Wetzlar, Germany).

2.7. Transmission electron microscopy (TEM) analysis

THP-1 cells (1×10^5 cells/well) were primed with PMA on a Lab-Tek II Chambered Coverglass and incubated for 6 h with 100 μg/mL mSP1000. They were then fixed in 2.5% glutaraldehyde followed by 1.5% osmium tetraoxide. The fixed cells were dehydrated and embedded in EPON resin. Ultrathin sections were stained with lead citrate and observed by TEM.

2.8. Flow cytometry

THP-1 cells (7×10^5 cells/well) were primed with PMA on 6-well plates and treated with 100 μg/mL mSP1000s for 6 h at 37 °C or 4 °C. After the treatment, cells were detached from the tissue culture plates by incubation with trypsin. Cells were then washed and evaluated in accordance with the Fluorescence-1 (FL-1) parameter using a FACSCalibur flow cytometer (Becton Dickinson, Franklin Lakes, NJ) and Flow Jo software (Three Star, Ashland, OR). Cells were gated to exclude SPs and small cell debris (low forward scatter). Cells with increased FL-1 fluorescence were expressed as a percentage of the maximum number (50,000) of gated cells.

2.9. Reverse transcription polymerase chain reaction (RT-PCR)

THP-1 cells (7×10^5 cells/well) were primed with PMA on 6-well plates and treated with 100 μg/mL mSP1000s for 3 h. After the treatment, total RNA was extracted from the cells by using Sepasol RNA-1 Super (Nacalai Tesque, Kyoto, Japan) in accordance with the manufacturer's instructions. Extracted RNA was reverse-transcribed with SuperScript III (Invitrogen). Synthesized cDNA was amplified by PCR using *Taq* DNA polymerase (Toyobo, Osaka, Japan). The sequences of the specific primers for IL-1β and GAPDH were as follows: IL-1β (F), 5′-AGAAGAACCTATCTTCTTCGA-3′; IL-1β (R), 5′-ACTCTCCAGCTGTAGAGTG G-3′; GAPDH (F), 5′-GCAGGGGGGAGCCAAAAGGG-3′; and GAPDH (R), 5′-TGCCAGCCCCAGCGTCAAAG-3′. After denaturation for 2 min at 95 °C, 20 cycles of three sequential steps—denaturation for 30 s at 95 °C, annealing for 30 s at 60 °C, and extension for 60 s at 72 °C—were performed, ending with a final extension step for 5 min at 72 °C. The PCR products were electrophoresed through a 2% agarose gel, stained with ethidium bromide, and visualized under ultraviolet radiation.

2.10. Observation of activated NLRP3 inflammasome

PMA-primed THP-1 cells were transiently transfected with the plasmid encoding cyan fluorescent protein (CFP)–ASC fusion protein (CFP–ASC) by using ExGen500 *in vitro* transfection agent (Fermentas, Baltimore, MD) in accordance with the manufacturer's instructions [25]. In brief, THP-1 cells (1×10^5 cells/well) were primed with PMA on Lab-Tek II Chambered Coverglass. The cells were then incubated for 60 h in 550 μL of cell culture medium containing the CFP–ASC plasmid (2 μg) – ExGen500 (50 μL) complex. The cells were washed and then treated with 100 μg/mL unmodified mSP1000 for 4 h. After the treatment, the cells were washed and then fixed with 4% paraformaldehyde. They were then mounted with Prolong

Gold Antifade Reagent (Invitrogen). Fluorescence was observed under a confocal laser scanning microscope.

2.11. Evaluation of reactive oxygen species (ROS) production

THP-1 cells (3×10^4 cells/well) were primed with PMA on 96-well black plates (Nunc) and treated with 100 μg/mL mSP1000s for 24 h. The cells were then incubated with 10 μM 2′,7′-dichlorodihydrofluorescein diacetate, acetyl ester (H_2DCFDA; Invitrogen) for 45 min and washed with PBS. Fluorescence was measured at $OD_{485-530}$ using a multi-well spectrophotometer (Molecular Devices, Inc., Tokyo, Japan). ROS production intensity was calculated by using the following formula: ROS production intensity = fluorescence/cell viability. The ROS production intensity of untreated control cells was arbitrarily set to 100%.

2.12. Statistical analysis

All results are presented as means ± SD or SEM. Differences were compared by using Student's *t*-test or Bonferroni's method after ANOVA.

3. Results

3.1. IL-1β production of SPs

To assess the correlation between particle size and the inflammatory effect of SPs, we examined the levels of IL-1β production induced by SPs in THP-1 macrophage-like cells (Fig. 1 A, B). First, we used unmodified SPs of five diameters between 30 and 1000 nm (unmodified nSP30, nSP50, nSP70, and nSP300, and unmodified mSP1000). The mean secondary particle diameters of each SP, measured by Zetasizer, were 33, 44, 79, 326, and 945 nm, respectively (data not shown). We already confirmed that these silica particles were smooth-surfaced spheres and well-dispersing by transmission electron microscopy (data not shown). We incubated THP-1 cells with SPs of each size for 6 h and then analyzed the levels of IL-1β in the culture supernatant. Unmodified mSP1000 induced significantly higher IL-1β production than PBS control, whereas the other, smaller SPs did not induce IL-1β production (Fig. 1A).

Next, to assess the correlation between surface modification and the inflammatory effect of SPs, we used mSP1000s with various surface-modification groups (unmodified, or with an added -COOH, $-NH_2$, $-SO_3H$, or -CHO group) (Fig. 1B). The mean secondary particle diameters of each type of mSP1000 were 945, 1022, 958, 1023, and 969 nm, respectively (data not shown). We incubated THP-1 cells with these surface-modified particles for 6 or 24 h and then examined the IL-1β production levels. Unmodified mSP1000 induced significantly greater IL-1β production than did the medium controls at both 6 and 24 h, whereas the surface-modified mSP1000s induced low levels of IL-1β production (Fig. 1B). The rank order of IL-1β production levels was unmodified mSP1000 > $-COOH > -NH_2 = -SO_3H = -CHO$. Furthermore, we evaluated the inflammatory effect of each type of mSP1000 *in vivo*. We intraperitoneally injected mSP1000s into C57CL/6 mice and analyzed the total number of live cells in the PCLF, because inflammation induces local infiltration by various inflammatory cells (Fig. 1C) [28]. The unmodified mSP1000 induced significantly greater cell migration than did the PBS control. The surface-modified mSP1000s did not induce cell accumulation beyond the control level. The rank order of the *in vivo* inflammatory effect was tended to the same as that of IL-1β production *in vitro*. These results indicate that appropriate surface modification with a functional group suppresses the inflammatory effect of unmodified mSP1000.

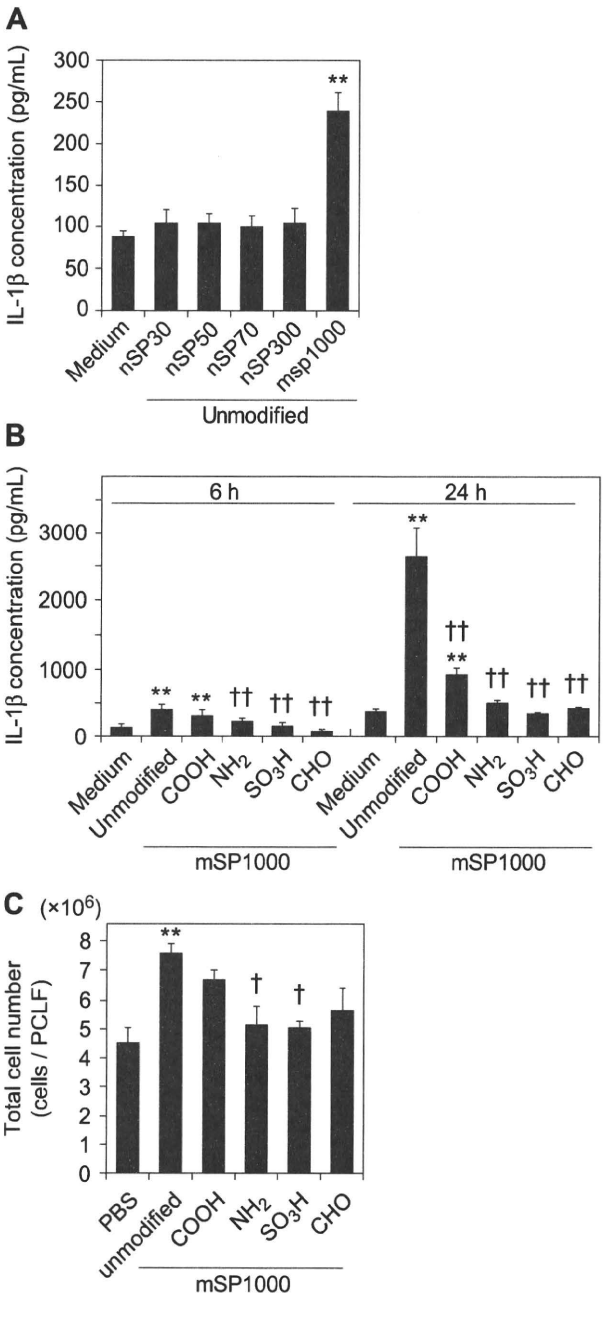

Fig. 1. Correlation between SP characteristics and inflammatory effects *in vitro* and *in vivo*. (A, B) IL-1β production levels in response to SPs of various sizes or with various surface modifications. PMA-primed THP-1 cells were treated with (A) unmodified SPs (30 nm–1000 nm) or (B) unmodified mSP1000, or mSP1000s modified with -COOH, $-NH_2$, $-SO_3H$, or -CHO for 6 or 24 h. IL-1β production levels in the culture supernatant were measured by ELISA. Data represent means ± SD ($n = 5$; $^{**}P < 0.01$ versus value for medium control, $^{\dagger\dagger}P < 0.01$ versus value for unmodified mSP1000, ANOVA). (C) Inflammatory effects of mSP1000s *in vivo*. Mice were intraperitoneally injected with PBS or with 1 mg of one type of mSP1000, and the total numbers of live cells in the PCLF were evaluated after 6 h. Data represent means ± SEM ($n = 5$; $^{*}P < 0.05$ versus value for PBS control, $^{\dagger}P < 0.05$ versus value for unmodified mSP1000, ANOVA).

3.2. Phagocytosis of mSP1000s

Through their phagocytic activity, macrophages play an important role in determining the bio-persistence of foreign particles and initiating inflammatory responses, including IL-1β production [29]. Therefore, to investigate whether mSP1000-induced IL-1β production was triggered by phagocytosis, we pretreated THP-1 cells with cytochalasin D, a well-characterized inhibitor of phagocytosis that impairs actin filament assembly (Fig. 2A). We then

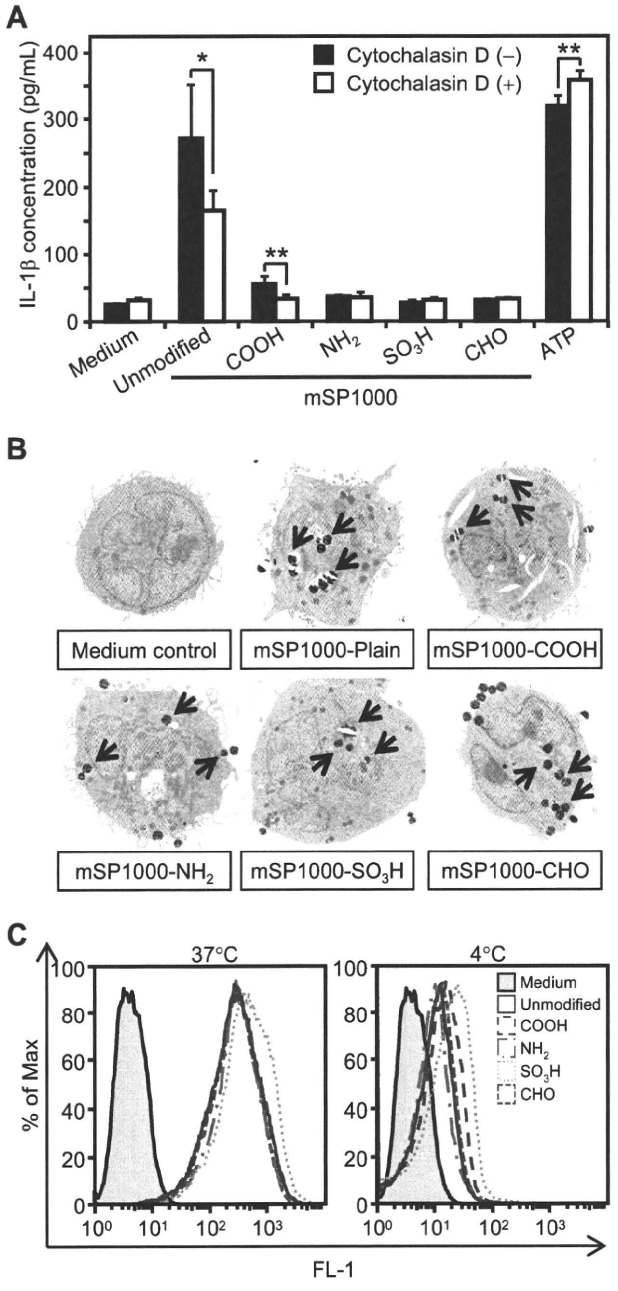

Fig. 2. Phagocytosis is a first signal for mSP1000-induced IL-1β production. (A) Involvement of phagocytosis in mSP1000-induced IL-1β production. PMA-primed THP-1 cells were treated with mSP1000s or ATP for 6 h in the absence (black bars) or presence (white bars) of cytochalasin D (5 μM). IL-1β production levels were then measured by ELISA. Data represent means ± SD ($n = 5$; $^*P < 0.05$, $^{**}P < 0.01$ versus value for cytochalasin D [−] control within each treatment pair, *t*-test). (B) TEM analysis of mSP1000s. PMA-primed THP-1 cells were treated with mSP1000s for 6 h. Cells were then observed by TEM. Arrows indicate ingested mSP1000s. (C) Flow cytometry of FITC-mSP1000s taken up into PMA-primed THP-1 cells. Cells were treated with mSP1000s and incubated for 6 h at 37 °C (left) or 4 °C (right). Data were analyzed by using the FL-1 parameter for green fluorescence.

treated the cells with mSP1000s or ATP, a well-known caspase-1 activator without cellular internalization. The cytochalasin D abolished the mSP1000-induced IL-1β production, whereas the response to ATP was unaffected (Fig. 2A). These results indicate that cellular ingestion of mSP1000s might be the first signal in the inflammatory response. We then speculated that the reduction in IL-1β production through surface modification of mSP1000s resulted from a change in the particle uptake frequency. We used TEM and flow cytometry to evaluate the frequency of uptake of mSP1000s (Fig. 2B, C). TEM analysis clearly showed that both the modified and unmodified mSP1000s were taken up by THP-1 cells (Fig. 2B). Furthermore, flow-cytometric analysis using FITC-conjugated mSP1000s showed that the frequencies of cellular ingestion of modified and unmodified mSP1000s were comparable at 37 °C (Fig. 2C). We also noted that the intensity of FITC-derived fluorescence was almost the same among the different types of mSP1000, and that the increase in the FL-1 signals was dose dependent (data not shown). These results collectively indicate that the unmodified and surface-modified mSP1000s were taken up with similar frequencies equally into the THP-1 cells by actin-dependent phagocytosis, independent of the type of modification group. Therefore, we considered that the difference in IL-1β production levels among mSP1000s was resulted from the signaling intensity in the IL-1β production cascade after ingestion of the mSP1000s by the cell.

3.3. Activation of caspase-1 by mSP1000s

IL-1β production is regulated by pro-IL-1β mRNA expression levels and by caspase-1 activity [17,22,23]. Therefore, to examine the mechanisms of the reduction in IL-1β production by surface modification, we used semi-quantitative RT-PCR to investigate the expression levels of pro-IL-1β mRNA in THP-1 cells treated with each type of mSP1000 (Fig. 3A). There were no significant differences in the expression levels of pro-IL-1β mRNA between cells treated with unmodified and modified mSP1000s. We then tested whether the reduction in IL-1β production by surface modification of mSP1000s resulted from changes in caspase-1 activity induced by mSP1000s. To investigate the association of caspase-1 activity with mSP1000-induced IL-1β production, we treated cells with mSP1000s in the presence of a caspase-1 specific inhibitor, zYVAD-fmk, and analyzed the IL-1β production levels (Fig. 3B). The results showed that zYVAD-fmk almost completely abrogated the IL-1β production induced by mSP1000s. These results collectively indicate that the IL-1β production induced by unmodified mSP1000 depend on the activation of caspase-1. Furthermore, it was speculated that the surface-modified mSP1000s induced little caspase-1 activation.

3.4. Activation of NLRP3 inflammasome by unmodified mSP1000

Recently, NLRP3 inflammasome was identified as the principal activator of caspase-1 in response to several types of danger signal [17,22,23]. To examine whether unmodified mSP1000 exerts their inflammatory potential through NLRP3 inflammasome, we examined the activation of NLRP3 inflammasome on THP-1 cells after treatment with unmodified mSP1000 (Fig. 4) [13,23]. We transiently transfected THP-1 cells with a plasmid expressing CFP–ASC fusion protein. ASC forms large oligomers after its activation, and the clustering of CFP–ASC can be used as an "optical reporter" of the activation of NLRP3 inflammasome [25,30]. Under baseline conditions CFP–ASC fluorescence was evenly distributed in the cytoplasm. Four hours after treatment with unmodified mSP1000, we detected bright fluorescent clusters of CFP–ASC in the cytoplasm. These clusters were not detected in non-transfected THP-1 cells treated with unmodified mSP1000, indicating that the clusters represented cytoplasmic aggregates of activated ASC in NLRP3 inflammasome. These results indicate that mSP1000-induced IL-1β production is mediated by the activation of NLRP3 inflammasome.

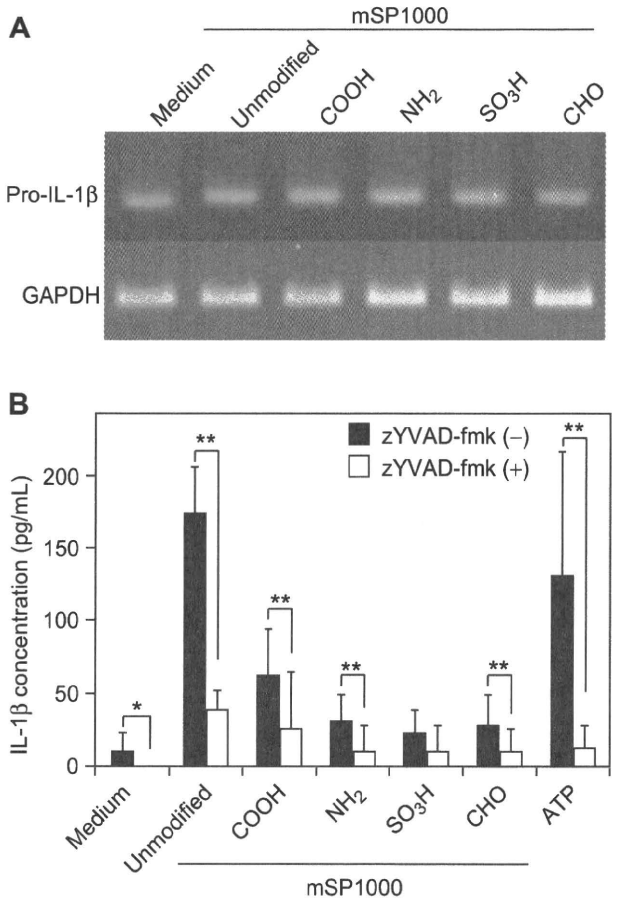

Fig. 3. Differences in levels of IL-1β production induced by each type of mSP1000 depend on caspase-1 activation. (A) Pro-IL-1β mRNA expression levels in mSP1000-treated cells. PMA-primed THP-1 cells were treated with mSP1000s and incubated for 3 h. Then, total RNA was isolated, and RT-PCR was performed with primers specific for IL-1β (top) or GAPDH (bottom). (B) Involvement of caspase-1 activity in mSP1000-induced IL-1β production. PMA-primed THP-1 cells were treated with each type of mSP1000 or with ATP for 6 h in the absence (black bars) or presence (white bars) of zYVAD-fmk (10 μM). IL-1β production levels were analyzed by ELISA. Data represent means ± SD ($n = 5$; $^{*}P < 0.05$, $^{**}P < 0.01$ versus value for zYVAD-fmk [−] control within each treatment pair, *t*-test).

3.5. Endosomal rupture and cathepsin B leakage

With crystalline silica, Hornung et al. reported that endosomal rupture plays a central role in activation of NLRP3 inflammasome followed by leakage of cathepsin B, a endosomal hydrolytic enzyme [20]. To investigate the mechanisms of IL-1β production induced by mSP1000, we compared the frequency of endosomal rupture and subsequent cathepsin B leakage among each type of mSP1000, using Alexa Fluor 594 dextran as an endocytic compartment marker [31]. Mature endosomes incorporating dextran are observed as dotted forms, and the spread of dextran into the cytoplasm is recognized as an indicator of endosomal rupture [20]. We incubated THP-1 cells with dextran and different types of mSP1000 and observed the behavior of the ingested dextran by confocal microscopy (Fig. 5A). Upon treatment of the cells with unmodified mSP1000, we detected the obvious spread of dextran throughout the cytosol, unlike in untreated control cells, indicating that unmodified mSP1000 induced endosomal rupture (Fig. 5A). In contrast, the degree of endosomal rupture was decreased in cells treated with surface-modified mSP1000s, while mSP1000–COOH induced endosomal rupture to some extent as the IL-1β production levels (Fig. 5A). To investigate whether cathepsin B was involved in mSP1000-induced IL-1β production, we treated cells with mSP1000s in the presence of a specific inhibitor of vacuolar H^+-ATPase (bafilomycin A_1), which is needed to activate cathepsin B and a membrane-permeable cathepsin B-specific chemical inhibitor (CA-074-Me). Both inhibitors almost completely suppressed IL-1β production induced by mSP1000s (Fig. 5B and C). These results collectively suggest that the activation of NLRP3 inflammasome and subsequent IL-1β production induced by mSP1000s are triggered by active cathepsin B leakage into the cytoplasm. Furthermore, they suggest that the reduction in IL-1β production by surface modification of mSP1000s results from a reduction in the frequency of mSP1000-induced endosomal rupture and subsequent cathepsin B leakage.

3.6. ROS production of mSP1000s

Another study has shown that ROS, in addition to cathepsin B, plays a crucial role in NLRP3 activation [13,19]. To investigate whether mSP1000-induced activation of NLRP3 inflammasome is dependent on ROS, we measured the levels of ROS in mSP1000-treated THP-1 cells by H_2DCFDA [32]. Treatment of THP-1 cells with unmodified mSP1000, but not with surface-modified SP1000s, significantly enhanced ROS production compared with that in the medium control (Fig. 6A). To confirm the involvement of ROS in mSP1000-induced IL-1β production, we evaluated the levels of IL-1β induced by mSP1000s in the presence of a broad ROS scavenger, BHA, or a specific inhibitor of NADPH oxidase, DPI. NADPH oxidase is an important enzymatic source for the production of ROS [33]. We confirmed that both BHA and DPI significantly suppressed unmodified mSP1000–induced IL-1β production (Fig. 6B and C). These results indicate that, in addition to cathepsin B, mSP1000-induced ROS play an important role in NLRP3 activation.

We then examined the association between mSP1000-induced ROS production and endosomal rupture. We incubated cells with dextran and unmodified mSP1000 in the presence of BHA and observed the behavior of the dextran as a reflection of endosomal morphology. The endosomal rupture induced by unmodified mSP1000 was almost completely suppressed by BHA (Fig. 6D). These observations collectively suggest that ROS production induced by phagocytosis of unmodified mSP1000 triggered endosomal rupture followed by the activation of NLRP3 inflammasome and subsequent IL-1β production. Furthermore, they also strongly indicate that the reduction in ROS production by surface modification attributes to the decrement of the IL-1β production seen with unmodified mSP1000.

3.7. Cell death by unmodified mSP1000

We reported previously that mSP1000-induced cell death is dependent in part on ROS but independent of caspase-1, -3, -4, and -7, and we also showed that surface modification of mSP1000 significantly suppresses particle cytotoxicity [34]. Here, we speculated that mSP1000-induced cell death was dependent on cathepsin B leakage or on IL-1β signaling triggered by ROS production. Therefore, to investigate the association of cathepsin B and IL-1β signaling with mSP1000-induced cell death, we treated THP-1 cells with unmodified mSP1000 in the presence or absence of CA-074-Me, bafilomycin A_1, or zYVAD-fmk. CA-074-Me and bafilomycin A_1, but not zYVAD-fmk, significantly suppressed the cytotoxicity of unmodified mSP1000 (Fig. 6E). These findings indicate that unmodified mSP1000–induced cell death depends in part on ROS and active cathepsin B but is independent of caspases and IL-1β signals.

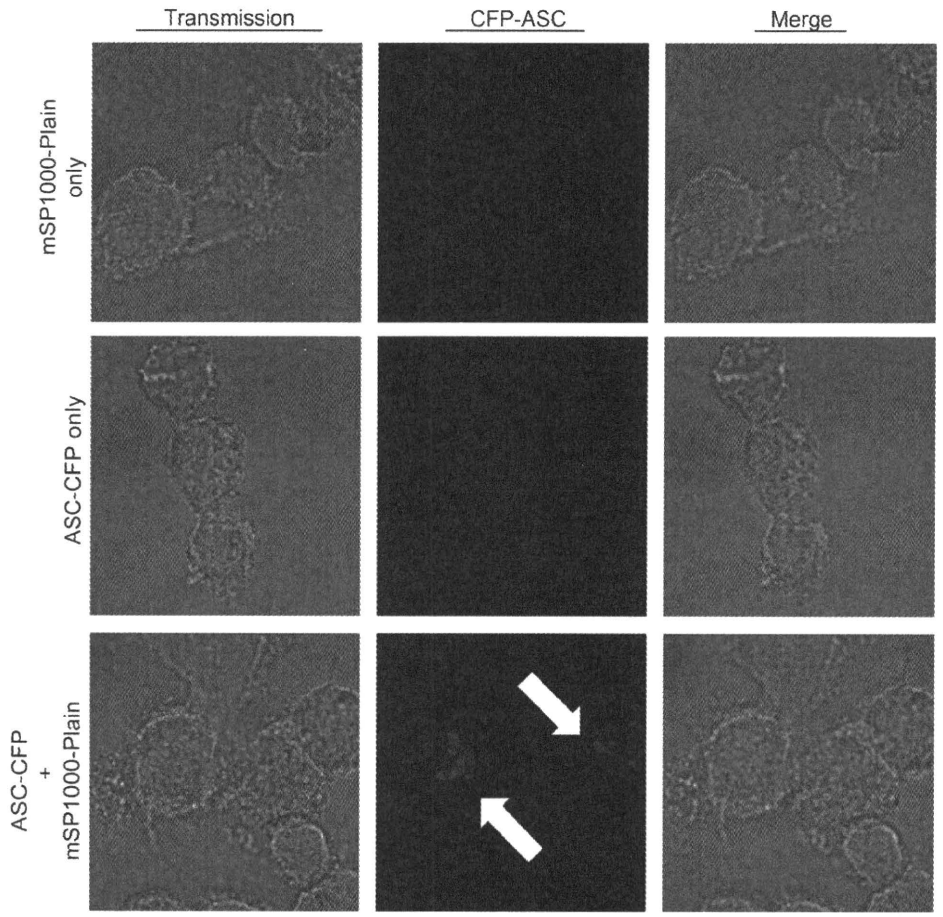

Fig. 4. Unmodified mSP1000–induced IL-1β production is mediated by activation of NALP3 inflammasome. PMA-primed THP-1 cells transiently transfected with CFP–ASC were treated with unmodified mSP1000. The cells were then observed by confocal microscopy. Treated with unmodified mSP1000 alone (top); untreated but transfected with CFP–ASC (middle); or treated with unmodified mSP1000 and transfected with CFP–ASC (bottom). Arrows indicate clusters of CFP–ASC (blue).

4. Discussion

Our goal was to elucidate the mechanisms of the inflammatory effects induced by SPs and to provide basic information for the creation of safe and effective SPs. To achieve these purposes, we focused on the IL-1β production induced by SPs, because IL-1β production is currently considered to play an important role in the initial inflammatory responses that lead to asbestosis and silicosis [19]. Our results provided evidence that unmodified mSP1000, but not smaller SPs, induces significant IL-1β production by THP-1 cells. Although the detailed mechanisms of this particle-size dependency in IL-1β production were unclear, we speculate that there are differences in the intracellular behavior of SPs and in the signaling pathways, and cytokine production patterns induced by SPs. Consistent with our hypothesis, our unpublished data showed that mSP1000s and the smaller SPs induce different inflammatory cytokine and chemokine production profiles (data not shown). Furthermore, many reports have shown that nanosized SPs induce inflammation *in vivo*. Therefore, we consider that it is also necessary to investigate the cytokine and chemokine production profiles induced by SPs of various sizes.

We then examined the effects of surface modification on mSP1000-induced IL-1β production, because it has become evident that surface properties are important factors in the biological effects of particles [14,15]. Interestingly, although unmodified and surface-modified mSP1000s were taken up equally, surface-modified mSP1000s induce little or no IL-1β production (Fig. 1B). The *in vivo* inflammatory effect was similarly reduced by surface modification of mSP1000s (Fig. 1C). We consider these results important to the creation of safe SPs.

Next, we examined the mechanisms of IL-1β production induced by mSP1000s to elucidate why surface modification reduced IL-1β production. First, we revealed that mSP1000-induced IL-1β production depends on the activation of NLRP3 inflammasome by using CFP–ASC fusion protein (Fig. 4). Some reports showed that other inflammasomes such as NLRP1 could activate caspase-1 in an ASC-dependent way [35]. Therefore we will need to confirm a specific role for NLRP3 in IL-1β production induced by mSP1000s by using siRNA of NLRP3 in future. A recent study showed that NLRP3 inflammasome mediated IL-1β production is associated with fever syndromes characterized by spontaneous inflammation [21]. In fact, the IL-1β receptor antagonist anakinra has been successfully used to treat patients suffering from inflammatory diseases, indicating that these patients have underlying increased IL-1β production [36,37]. However, the mechanisms of NLRP3 activation remain unclear, and therefore the definitive target to be overcome for the creation of safe materials is still unknown. Recently, different groups separately reported that cathepsin B leakage after endosomal rupture, as well as cytoplasmic ROS, plays a crucial role in the activation of NLRP3 inflammasome [13,20]. Consistent with these notions, we demonstrated here that mSP1000-induced IL-1β production is mediated by cathepsin B and

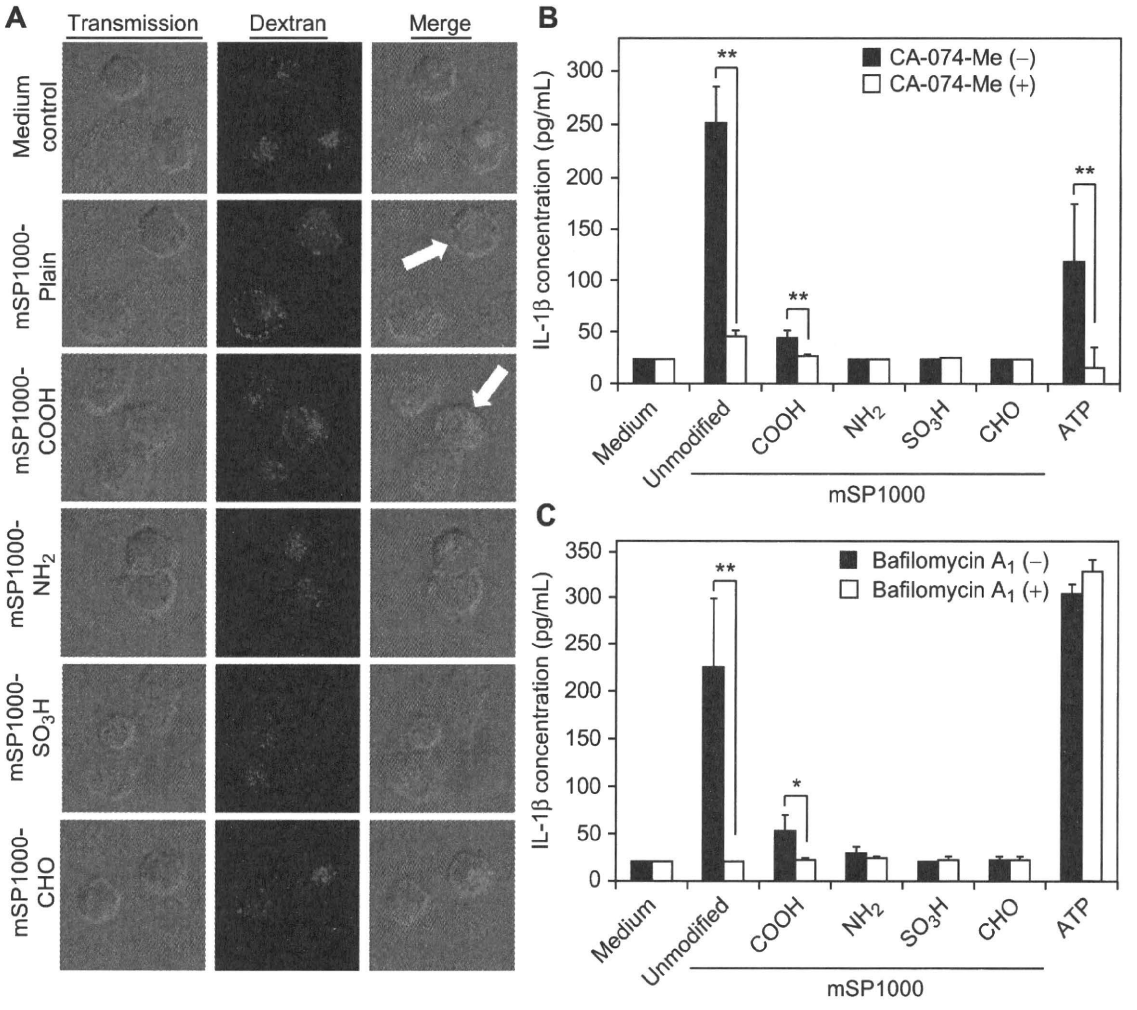

Fig. 5. mSP1000-induced IL-1β production is mediated by endosomal rupture. (A) Confocal microscopy of endosomal morphology. PMA-primed THP-1 cells were incubated with Alexa Fluor 594–conjugated dextran (red) and each type of mSP1000 for 6 h. The cells were then observed by confocal microscopy. Arrows show cells with spread of dextran into the cytoplasm, indicating endosomal rupture. (B, C) Involvement of cathepsin B in mSP1000-induced IL-1β production. PMA-primed THP-1 cells were treated with each type of mSP1000 or with ATP for 6 h in the absence (black bars) or presence (white bars) of (B) CA-074-Me (2 μM) or (C) bafilomycin A_1 (250 nM). Data represent means ± SD ($n = 5$; $^*P < 0.05$, $^{**}P < 0.01$ versus value for inhibitor [–] control within each treatment pair, *t*-test).

ROS (Figs. 5 and 6). However, it was unclear whether ROS and cathepsin B activate NLRP3 inflammasome separately or in a coordinated manner, and it was also unclear how endosomal rupture occurred. Use of a ROS inhibitor and surface-modified mSP1000s efficiently suppressed endosomal rupture (Fig. 6D). From these observations, we speculate that, with mSP1000 treatment, ROS trigger endosomal rupture and subsequent cathepsin B leakage into the cytosol, leading to the activation of NLRP3 inflammasome (Fig. 7). Our hypothesis is consistent with some reports suggesting that ROS trigger destabilization of the lysosomal membrane by membrane lipid oxidation [38].

In contrast, some reports have suggested that, in the case of crystalline silica, the reactive particle surface interacts with phagolysosomal membranes, leading to the release of endosomal enzymes into the cytosol after phagocytosis [39–41]. These contradictory findings suggest that various materials induce biological effects by different mechanisms in response to differences in particle characteristics. However, it remains unclear why the surface modification of mSP1000 reduced ROS production. It is possible that inappropriate surface modification induces an inflammatory effect stronger that of unmodified SP. We consider that further studies of the relationship between surface characteristics and bio-effect are necessary for the development of safe and effective materials. In this report, we found that DPI, an inhibitor of NADPH oxidase, significantly suppressed mSP1000-induced IL-1β production (Fig. 6C). NADPH oxidase is activated by the assembly of membrane lipids at local sites on the cellular surface and in the cytoplasm where the particles attach [42,43]. At this point, the silanol group (Si–OH) induces binding of the particles to membranes [44,45]. Therefore, we speculate that surface modification of mSP1000 masks the silanol group from the surface of the mSP1000 and blocks subsequent NADPH oxidase activation.

On the other hand, SP-induced cell death is also a critical obstacle, because macrophages play a central role in host defense systems. In 2007, Willingham et al. proposed a novel cell death pathway called pyronecrosis [46]. Induction of pyronecrosis is not dependent on IL-1β signaling or caspase-1 activity, although it requires the presence of the inflammasome component ASC and cathepsin B [46–48]. Our data suggested that mSP1000-induced cell death is independent of caspase-1 and IL-1β signaling but

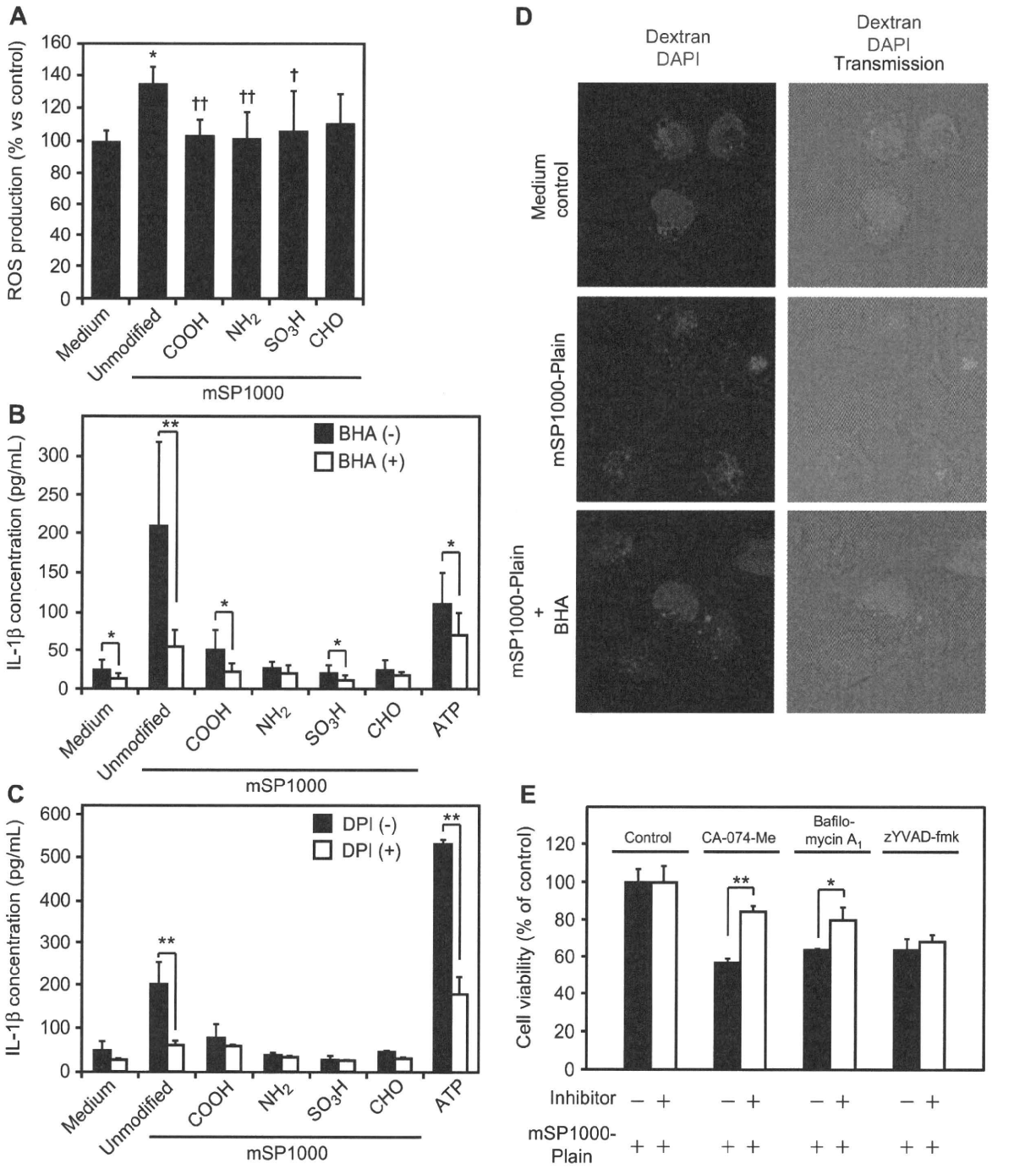

Fig. 6. Unmodified mSP1000–induced ROS production induces endosomal rupture and subsequent IL-1β production. (A) ROS production levels in PMA-primed THP-1 cells. Cells were treated with each type of mSP1000 for 24 h and incubated with H_2DCFDA (10 μM) for 45 min. Fluorescence was then measured at $OD_{485-530}$. ROS production intensity was calculated by the formula ROS production intensity = fluorescence/number of live cells. ROS production intensity of untreated control cells was arbitrarily set to 100%. Data represent means ± SD ($n = 5$; $^{*}P < 0.05$ versus value for PBS control, $^{\dagger}P < 0.05$, $^{\dagger\dagger}P < 0.01$ versus value for unmodified mSP1000, ANOVA). (B, C) Involvement of ROS in mSP1000-induced IL-1β production. PMA-primed THP-1 cells were treated with each type of mSP1000 or with ATP for 6 h in the absence (black bars) or presence (white bars) of (B) BHA (150 μM) or (C) DPI (60 μM), and IL-1β production levels were measured by ELISA. (D) Confocal microscopy of endosomal morphology. PMA-primed THP-1 cells were incubated with Alexa Fluor 594–conjugated dextran (red) and unmodified mSP1000 for 6 h in the presence (bottom) or absence (middle) of BHA (150 μM). Cells were then observed by confocal microscopy. Arrows indicate cells with spread of dextran into the cytoplasm. (E) Involvement of cathepsin B and caspase-1 in unmodified mSP1000–induced cytotoxicity. PMA-primed THP-1 cells were treated with unmodified mSP1000 for 24 h in the absence (black bars) or presence (white bars) of CA-074-Me (2 μM), bafilomycin A_1 (250 nM), or zYVAD-fmk (10 μM). Cell viability was measured by methylene blue assay. Data represent means ± SD ($n = 5$; $^{*}P < 0.05$, $^{**}P < 0.01$ versus value for inhibitor [−] control within each treatment pair, *t*-test).

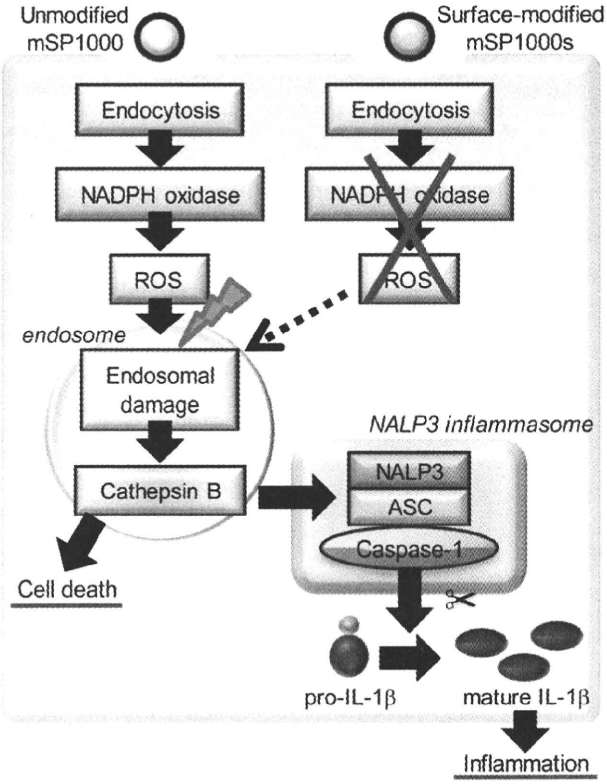

Fig. 7. Model of mSP1000-induced IL-1β maturation pathways. Unmodified mSP1000–induced IL-1β maturation is mediated by phagocytosis, activation of NADPH oxidase, ROS production, endosomal rupture, active cathepsin B leakage, assembly of NALP3 inflammasome, and caspase-1 activation. Surface-modified mSP1000s do not activate NADPH oxidase or ROS production, although they are taken up at the same rate as unmodified mSP1000.

dependent on cathepsin B (Fig. 6E) with the ASC assembly (Fig. 4), which means that unmodified mSP1000–induced cell death might occur by pyronecrosis. Pyronecrosis is considered to elicit substantial inflammation and to affect the local environment, whereas apoptosis is widely accepted as non-inflammatory cell death without effects around the dying cells [48]. Thus, pyronecrosis is likely to contribute substantially to the disease state in patients with inflammatory diseases.

We revealed here that SP-induced ROS act as an important upstream signal in the NLRP3 activation pathway. Moreover, we showed that modification of mSP1000s with functional groups suppressed their inflammatory effects. We have since obtained similar results with nanosized particles (nSP70) (unpublished data). These results support our hypothesis that appropriate surface modification of SPs suppresses their inflammatory effect. However, we speculate that blind modification could exacerbate the inflammatory effect, and we consider that an analysis of the mechanisms of the phenomena reported here is necessary.

5. Conclusions

We reveal here that unmodified mSP1000–induced IL-1β production is mediated by the activation of NADPH oxidase, ROS production, endosomal rupture, active cathepsin B leakage, assembly of NLRP3 inflammasome, and caspase-1 activation. Furthermore, by surface modification with functional groups, we successfully suppressed unmodified mSP1000–induced ROS production, an upstream signal in the NLRP3 activation pathway, and the subsequent inflammatory responses or cell death. We consider that further studies of the relationship between surface characteristics and biological effects would lead to the development of safe and effective SPs.

Acknowledgements

The authors declare that they have no conflict of interests. We thank Dr. D.T. Golenbock (Department of Infectious Diseases and Immunology, University of Massachusetts Medical School) for providing CFP–ASC plasmid. This study was supported in part by grants from the Ministry of Health, Labor, and Welfare of Japan; by the Ministry of the Environment of Japan; and by the Global COE Program "In Silico Medicine" at Osaka University.

Appendix

Figures with essential color discrimination. Figs. 2, 4–7 in this article are difficult to interpret in black and white. The full color images can be found in the on-line version, at doi:10.1016/j.biomaterials.2010.05.036.

References

[1] Mossman BT, Churg A. Mechanisms in the pathogenesis of asbestosis and silicosis. Am J Respir Crit Care Med 1998;157:1666–80.
[2] Huaux F. New developments in the understanding of immunology in silicosis. Curr Opin Allergy Clin Immunol 2007;7:168–73.
[3] Hirsch LR, Stafford RJ, Bankson JA, Sershen SR, Rivera B, Price RE, et al. Nanoshell-mediated near-infrared thermal therapy of tumors under magnetic resonance guidance. Proc Natl Acad Sci U S A 2003;100:13549–54.
[4] Bharali DJ, Klejbor I, Stachowiak EK, Dutta P, Roy I, Kaur N, et al. Organically modified silica nanoparticles: a nonviral vector for in vivo gene delivery and expression in the brain. Proc Natl Acad Sci U S A 2005;102:11539–44.
[5] Roy I, Ohulchanskyy TY, Bharali DJ, Pudavar HE, Mistretta RA, Kaur N, et al. Optical tracking of organically modified silica nanoparticles as DNA carriers: a nonviral, nanomedicine approach for gene delivery. Proc Natl Acad Sci U S A 2005;102:279–84.
[6] Bottini M, D'Annibale F, Magrini A, Cerignoli F, Arimura Y, Dawson MI, et al. Quantum dot-doped silica nanoparticles as probes for targeting of T-lymphocytes. Int J Nanomedicine 2007;2:227–33.
[7] Verraedt E, Pendela M, Adams E, Hoogmartens J, Martens JA. Controlled release of chlorhexidine from amorphous microporous silica. J Contr Release 2010;142:47–52.
[8] Wiethoff AJ, Reed KL, Webb TR, Warheit DB. Assessing the role of neutrophil apoptosis in the resolution of particle-induced pulmonary inflammation. Inhal Toxicol 2003;15:1231–46.
[9] Cho WS, Choi M, Han BS, Cho M, Oh J, Park K, et al. Inflammatory mediators induced by intratracheal instillation of ultrafine amorphous silica particles. Toxicol Lett 2007;175:24–33.
[10] Park EJ, Park K. Oxidative stress and pro-inflammatory responses induced by silica nanoparticles in vivo and in vitro. Toxicol Lett 2009;184:18–25.
[11] Akerman ME, Chan WC, Laakkonen P, Bhatia SN, Ruoslahti E. Nanocrystal targeting in vivo. Proc Natl Acad Sci U S A 2002;99:12617–21.
[12] Kirchner C, Liedl T, Kudera S, Pellegrino T, Munoz Javier A, Gaub HE, et al. Cytotoxicity of colloidal CdSe and CdSe/ZnS nanoparticles. Nano Lett 2005;5:331–8.
[13] Dostert C, Petrilli V, Van Bruggen R, Steele C, Mossman BT, Tschopp J. Innate immune activation through Nalp3 inflammasome sensing of asbestos and silica. Science 2008;320:674–7.
[14] Albrecht C, Schins RP, Hohr D, Becker A, Shi T, Knaapen AM, et al. Inflammatory time course after quartz instillation: role of tumor necrosis factor-alpha and particle surface. Am J Respir Cell Mol Biol 2004;31:292–301.
[15] He X, Nie H, Wang K, Tan W, Wu X, Zhang P. In vivo study of biodistribution and urinary excretion of surface-modified silica nanoparticles. Anal Chem 2008;80:9597–603.
[16] Waters KM, Masiello LM, Zangar RC, Tarasevich BJ, Karin NJ, Quesenberry RD, et al. Macrophage responses to silica nanoparticles are highly conserved across particle sizes. Toxicol Sci 2009;107:553–69.
[17] Dinarello CA. Interleukin-1 beta, interleukin-18, and the interleukin-1 beta converting enzyme. Ann N Y Acad Sci 1998;856:1–11.
[18] Petrilli V, Dostert C, Muruve DA, Tschopp J. The inflammasome: a danger sensing complex triggering innate immunity. Curr Opin Immunol 2007;19:615–22.

[19] Cassel SL, Eisenbarth SC, Iyer SS, Sadler JJ, Colegio OR, Tephly LA, et al. The Nalp3 inflammasome is essential for the development of silicosis. Proc Natl Acad Sci U S A 2008;105:9035–40.
[20] Hornung V, Bauernfeind F, Halle A, Samstad EO, Kono H, Rock KL, et al. Silica crystals and aluminum salts activate the NALP3 inflammasome through phagosomal destabilization. Nat Immunol 2008;9:847–56.
[21] Ting JP, Kastner DL, Hoffman HM. CATERPILLERs, pyrin and hereditary immunological disorders. Nat Rev Immunol 2006;6:183–95.
[22] Martinon F, Petrilli V, Mayor A, Tardivel A, Tschopp J. Gout-associated uric acid crystals activate the NALP3 inflammasome. Nature 2006;440:237–41.
[23] Agostini L, Martinon F, Burns K, McDermott MF, Hawkins PN, Tschopp J. NALP3 forms an IL-1beta-processing inflammasome with increased activity in Muckle-Wells autoinflammatory disorder. Immunity 2004;20:319–25.
[24] Mariathasan S, Weiss DS, Newton K, McBride J, O'Rourke K, Roose-Girma M, et al. Cryopyrin activates the inflammasome in response to toxins and ATP. Nature 2006;440:228–32.
[25] Halle A, Hornung V, Petzold GC, Stewart CR, Monks BG, Reinheckel T, et al. The NALP3 inflammasome is involved in the innate immune response to amyloid-beta. Nat Immunol 2008;9:857–65.
[26] Shio MT, Eisenbarth SC, Savaria M, Vinet AF, Bellemare MJ, Harder KW, et al. Malarial hemozoin activates the NLRP3 inflammasome through Lyn and Syk kinases. PLoS Pathog 2009;5:e1000559.
[27] Yoshioka Y, Watanabe H, Morishige T, Yao X, Ikemizu S, Nagao C, et al. Creation of lysine-deficient mutant lymphotoxin-alpha with receptor selectivity by using a phage display system. Biomaterials 2010;31:1935–43.
[28] Busuttil SJ, Ploplis VA, Castellino FJ, Tang L, Eaton JW, Plow EF. A central role for plasminogen in the inflammatory response to biomaterials. J Thromb Haemost 2004;2:1798–805.
[29] Chung EY, Kim SJ, Ma XJ. Regulation of cytokine production during phagocytosis of apoptotic cells. Cell Res 2006;16:154–61.
[30] Fernandes-Alnemri T, Wu J, Yu JW, Datta P, Miller B, Jankowski W, et al. The pyroptosome: a supramolecular assembly of ASC dimers mediating inflammatory cell death via caspase-1 activation. Cell Death Differ 2007;14:1590–604.
[31] Magalhaes AC, Baron GS, Lee KS, Steele-Mortimer O, Dorward D, Prado MA, et al. Uptake and neuritic transport of scrapie prion protein coincident with infection of neuronal cells. J Neurosci 2005;25:5207–16.
[32] Egler RA, Fernandes E, Rothermund K, Sereika S, de Souza-Pinto N, Jaruga P, et al. Regulation of reactive oxygen species, DNA damage, and c-Myc function by peroxiredoxin 1. Oncogene 2005;24:8038–50.
[33] Morel F, Doussiere J, Vignais PV. The superoxide-generating oxidase of phagocytic cells. Physiological, molecular and pathological aspects. Eur J Biochem 1991;201:523–46.
[34] Morishige A, Yoshioka Y, Inakura H, Tanabe A, Yao X, Tsunoda SI, et al. Cytotoxicity of amorphous silica particles against macrophage-like THP-1 cells depends on particle-size and surface properties. Pharmazie in press.
[35] Franchi L, Eigenbrod T, Munoz-Planillo R, Nunez G. The inflammasome: a caspase-1-activation platform that regulates immune responses and disease pathogenesis. Nat Immunol 2009;10:241–7.
[36] Piguet PF, Vesin C, Grau GE, Thompson RC. Interleukin 1 receptor antagonist (IL-1ra) prevents or cures pulmonary fibrosis elicited in mice by bleomycin or silica. Cytokine 1993;5:57–61.
[37] Hawkins PN, Lachmann HJ, McDermott MF. Interleukin-1-receptor antagonist in the Muckle-Wells syndrome. N Engl J Med 2003;348:2583–4.
[38] Kurz T, Terman A, Gustafsson B, Brunk UT. Lysosomes and oxidative stress in aging and apoptosis. Biochim Biophys Acta 2008;1780:1291–303.
[39] Allison AC, Harington JS, Birbeck M. An examination of the cytotoxic effects of silica on macrophages. J Exp Med 1966;124:141–54.
[40] Nadler S, Goldfischer S. The intracellular release of lysosomal contents in macrophages that have ingested silica. J Histochem Cytochem 1970;18:368–71.
[41] Erdogdu G, Hasirci V. An overview of the role of mineral solubility in silicosis and asbestosis. Environ Res 1998;78:38–42.
[42] Ng G, Sharma K, Ward SM, Desrosiers MD, Stephens LA, Schoel WM, et al. Receptor-independent, direct membrane binding leads to cell-surface lipid sorting and Syk kinase activation in dendritic cells. Immunity 2008;29:807–18.
[43] Kuijk LM, Beekman JM, Koster J, Waterham HR, Frenkel J, Coffer PJ. HMG-CoA reductase inhibition induces IL-1beta release through Rac1/PI3K/PKB-dependent caspase-1 activation. Blood 2008;112:3563–73.
[44] Nash T, Allison AC, Harington JS. Physico-chemical properties of silica in relation to its toxicity. Nature 1966;210:259–61.
[45] Pandurangi RS, Seehra MS, Razzaboni BL, Bolsaitis P. Surface and bulk infrared modes of crystalline and amorphous silica particles: a study of the relation of surface structure to cytotoxicity of respirable silica. Environ Health Perspect 1990;86:327–36.
[46] Willingham SB, Bergstralh DT, O'Connor W, Morrison AC, Taxman DJ, Duncan JA, et al. Microbial pathogen-induced necrotic cell death mediated by the inflammasome components CIAS1/cryopyrin/NLRP3 and ASC. Cell Host Microbe 2007;2:147–59.
[47] Fujisawa A, Kambe N, Saito M, Nishikomori R, Tanizaki H, Kanazawa N, et al. Disease-associated mutations in CIAS1 induce cathepsin B-dependent rapid cell death of human THP-1 monocytic cells. Blood 2007;109:2903–11.
[48] Ting JP, Willingham SB, Bergstralh DT. NLRs at the intersection of cell death and immunity. Nat Rev Immunol 2008;8:372–9.

日衛誌 (Jpn. J. Hyg.), 65, 487-492 (2010)

総　説

ミニ特集　第80回日本衛生学会
連携研究会：繊維・粒子状物質研究会

ナノマテリアルの安全確保に向けたNano-Safety Science研究

吉岡　靖雄[*1,2,3]，吉川　友章[*2,3]，堤　　康央[*1,2,3]

[*1]大阪大学臨床医工学融合研究教育センター
[*2]大阪大学大学院薬学研究科
[*3]独立行政法人医薬基盤研究所

Nano-Safety Science for Assuring the Safety of Nanomaterials

Yasuo YOSHIOKA[*1,2,3], Tomoaki YOSHIKAWA[*2,3] and Yasuo TSUTSUMI[*1,2,3]

[*1]*The Center for Advanced Medical Engineering and Informatics, Osaka University*
[*2]*Graduate School of Pharmaceutical Sciences, Osaka University*
[*3]*National Institute of Biomedical Innovation*

Abstract　**Developments in nanotechnology have fostered the widespread use of a diverse array of nanomaterials such as nanosilicas and carbon nanotubes. Nanomaterials are already being used in electronics, sunscreens, cosmetics, and medicines, because they have unique physicochemical properties, such as conductivity, strength, durability, and chemical reactivity. The advent of nanomaterials has also provided extraordinary opportunities for biomedical applications. However, the increasing use of nanomaterials has raised public concern about their potential risks to human health. In particular, recent reports have indicated that carbon nanotubes induce severe inflammation and mesothelioma-like lesions in mice. In this regard, we have attempted to elucidate the pharmacodynamics and safety of nanomaterials in order to develop novel, safe nanomaterials and to establish scientifically based regulations. In this review, we introduce our data on the safety of nanosilicas, particularly the relationships among their physical properties (predominant grain size, configuration, and surface charge), pharmacodynamics, and safety. Our study will help to improve the quality of human life by establishing standards for the safe use of nanomaterials.**

Key words: nanomaterial（ナノマテリアル），Nano-Safety Science，nanosilica（ナノシリカ）

はじめに

2000年1月に，当時の米国クリントン大統領が「国家ナノテクノロジー戦略」を発表し，大規模国家予算を投資したことが一つの起爆剤となり，ナノマテリアルの開発研究と生産，そして実用化が，国内外の産官学を問わず，多くの領域（医療，情報，環境，エネルギーなど）で急速に進展した。ナノマテリアルとは，少なくとも一次元の大きさが100 nm以下で製造された超微細材料と定義されている。このナノマテリアルは，従来までのサブミクロンサイズ以上（100 nm以上）の素材とは異なり，サイズ減少に伴う組織浸透性の増大や電子反応性の増大，重量あたりの表面積の増加などにより，抗酸化効果や紫外線遮蔽効果といった有用機能が格段に向上しており，我々の生活の質的向上に革命を起こすものと注目されている。そのため，種々の産業で夢の新素材になるものと期待されており，医薬品・食品・化粧品領域では，ナノシリカやナノ酸化チタン，フラーレン，白金ナノコロイド，ナノシルバーなどが，必須素材として既に上市されている（図1）。

一方で，ナノマテリアルの物性（サイズ，形状など）に起因した革新的機能が逆に，二面性を呈してしまい，

受付2010年7月31日，受理2010年7月31日
Reprint requests to: Yasuo YOSHIOKA, PhD
The Center for Advanced Medical Engineering and Informatics, Osaka University, 1-6 Yamadaoka, Suita, Osaka 565-0871, Japan
TEL: +81(6)6879-8177, FAX: +81(6)6879-8177
E-mail: yasuo@phs.osaka-u.ac.jp

物質名	国内生産量	用途
カーボンナノチューブ	120-140 t	電子材料
カーボンブラック	80万 t	タイヤ、自動車部品等
二酸化チタン	1450 t	化粧品、光触媒等
フラーレン	2 t	化粧品、スポーツ用品等
酸化亜鉛	480 t	化粧品等
非晶質シリカ	9万 t	食品、化粧品、インク、合成ゴム、タイヤ等

図1　主なナノマテリアルの生産量と用途。経済産業省のホームページから一部改変して転載。

サブミクロンサイズ以上の従来型素材では観察されない特徴的な毒性，所謂，ナノトックス（NanoTox）を発現してしまうことが世界的に懸念されている（1-3）。例えば，今後の詳細な検証が必要ではあるものの，カーボンナノチューブや酸化チタンの発がん性・起炎性など，健康被害を示唆する研究報告が相次いでいる（4-6）。そのため，経済協力開発機構（OECD）と連携しつつ，欧米各国などはナノマテリアルの開発やその利用を規制しようとする動きを加速している。我が国でも，厚生労働省や経済産業省，環境省，内閣府を中心にナノマテリアルの安全性評価研究が今，まさにスタートしたところである。

以上のNanoTox研究を推進するうえで考慮すべき点は，例えば医薬品・化粧品・食品の場合，老若男女・妊婦・胎児・乳幼児・病人を問わず，あらゆる世代のヒトが一生涯に渡って曝露され続けることにある。そのため，ナノマテリアルがごく僅かでも体内に吸収され，長期に渡って蓄積され続けると，安全性に大きな問題を招きかねない。しかし，NanoTox研究の大部分はハザード評価（毒性の有無）に偏重しているのが現状であり，肝心な“体内吸収性や体内／細胞内動態に関する情報”は，世界的に欠乏している。これは，従来までのサブミクロンサイズ以上の素材で積み重ねられてきた知見に基づき，ナノマテリアルの場合でも曝露されても吸収される筈がないだろうという誤った認識にも大きく影響されている。即ち，このままでは，ナノマテリアルの体内吸収性／体内動態に関する検討がなされぬまま，科学的根拠に乏しい無闇な使用規制が施行されてしまい，ナノマテリアルの有用性を享受した豊かな社会の構築や産業発展が阻害されてしまいかねない。従って，知財技術立国を目指す我が国としては，ナノマテリアルの開発・実用化を闇雲に規制するのではなく，ナノテクノロジーの恩恵を社会が最大限に享受できるよう，ナノ産業の育成や発展を強力に支援しつつ，一方で責任ある先進国，そして健康立国として，ナノマテリアルの安全性を高度に保障し，ヒトの健康環境を確保していかねばならない。すなわち，ナノマテリアルを活用した豊かな社会の構築のためにも，今こそ，どの程度我々はナノマテリアルに曝露されているのかといった曝露実態の解明や，生体内に取り込まれたナノマテリアルがどの程度組織に分布するのかといった定量的な体内動態評価，さらに，健康影響に及ぼす閾値追求など詳細な安全性評価が待望されている。

以上の背景を踏まえて我々は，安全なナノマテリアルの創製に向けた基盤情報の収集，使用指針の策定に向け，ナノマテリアルの物性・体内動態・安全性の3者連関を解析することで，健康影響発現に及ぼす閾値の追求・安全なナノマテリアルの設計指針の構築を図ってきた（6-11）。本稿では，我々の取り組みの中から，最も汎用されているナノマテリアルの一つである非晶質ナノシリカの安全性確保研究（我々は，安全なナノマテリアルの開発研究を推進する視点からNanoTox研究ではなく，Nano-Safety Science研究と呼んでいる）について，体内・細胞内動態解析と免疫毒性評価に焦点をあて紹介させて頂き，各方面の先生方からご意見・ご批判を仰ぎたい。

非晶質ナノシリカの物性と経皮吸収性との連関評価

非晶質ナノシリカの用途は非常に幅広く，日焼け止めやファンデーションなどの化粧品基材，歯磨き粉や歯の充填剤，食品の固結防止・流動化剤などの食品添加物として利用されている。また，非晶質ナノシリカは食品中に最大2%，化粧品におおよそ20%程度が配合されており，既に我々の生活に必須となっている。さらに近年では，非晶質ナノシリカのサイズダウンや分散性を向上する技術の開発が加速度的に進展しており，直径が2.5 nm程度のもの（所謂，サブナノサイズ）までも開発されつつあり，その使用量・適用範囲は増加の一途を辿っている。従って，非晶質ナノシリカの環境中への流出や廃棄，非晶質ナノシリカ含有製品の使用により，生体が経口，経肺，経皮など，様々な経路で非晶質ナノシリカに，意図的・非意図的な曝露を受ける機会が今後ますます増大していくことは想像に難くない。一方で，その安全性に関する検討は，他のナノマテリアルに比べて圧倒的に遅れているのが現状である。欧州化学物質生態毒性・毒性センターによれば，サブミクロンサイズ以上の非晶質シ

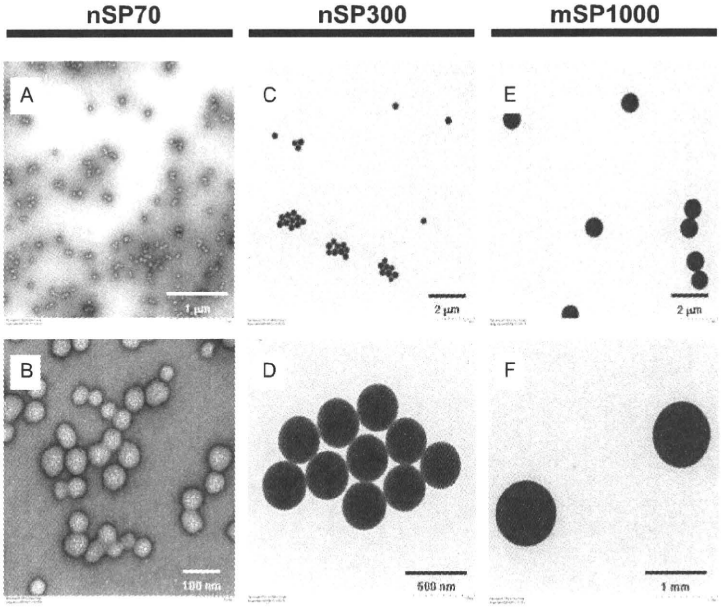

図2　非晶質シリカの電子顕微鏡写真。（A and B）直径70 nmのシリカ（nSP70），（C and D）直径300 nmのシリカ（nSP300），（E and F）直径1, 000 nmのシリカ（mSP1000）。

リカ（一次粒径は100 nm以下であっても，凝集体として，サブミクロンサイズ以上になる非晶質ナノシリカを含む）の安全性に問題は無いと報告されている（12）。しかし，この報告は，昨今の分散性に優れた100 nm以下の非晶質ナノシリカの安全性を保証するものではない。特に，100 nm以下の分散性の高い素材に関しては，体内に吸収される可能性が世界的に懸念されており，この点に関する検討が急務となっている。

そこで本研究では，まず，分散性が極めて高い非晶質シリカを用いて，経皮吸収性・体内動態と粒子サイズとの連関を検討した。本研究では，一次粒径が70 nmの非晶質ナノシリカ（nSP70）及び，粒子径300 nm，1, 000 nmの従来型非晶質シリカ（nSP300，mSP1000）を実験に用いた（現在は，30 nm，50 nmの非晶質ナノシリカやサブナノサイズのものも使用しているが，これらに関しては今後報告させて頂く）。図2に非晶質シリカの透過型電子顕微鏡（TEM）写真を示す。いずれの粒子も非常に滑らかな形状をした粒子であり，一次／二次粒子径もカタログ値とほぼ同等であった。続いて，nSP70，nSP300，mSP1000をマウス耳介に塗布した際の経皮吸収性を評価した。各非晶質シリカをマウスに5日間あるいは28日間連続経皮塗布し，投与局所および所属リンパ節，主要組織への移行をTEMにより観察した。その結果，nSP70が角質層を通過して表皮や真皮層にまで到達し，さらに，所属リンパ節・脾臓や脳内にまで移行することが明らかとなった。特に，リンパ節・脾臓では，リンパ球や貪食細胞であるマクロファージに多く取り込まれることが判明した。なお，従来までのサブミクロンサイズ以上の非晶質シリカであるnSP300やmSP1000は，表皮層にすら到達しないこと（即ち，高度に安全であること）を確認している。現在は，経口・経鼻・経肺曝露により，nSP70が投与部位の免疫担当細胞に多く取り込まれるだけでなく，生体内にも吸収されることを明らかとしつつあり，今後より詳細な体内動態を明らかにできるものと考えている。

そこで次に，各非晶質シリカをマウス尾静脈より投与し，非晶質ナノシリカが全身循環した際の動態および生体影響を評価した。まず，種々の粒子径の非晶質シリカの体内動態を蛍光イメージングならびにTEM解析により評価したところ，nSP300とmSP1000は胆嚢に局在する一方で，nSP70は肝臓全体へ速やかに分布することが明らかとなった（図3）。また，nSP300とmSP1000は肝実質細胞には殆ど移行しないにも関わらず，nSP70は肝実質細胞へ移行し，最終的に核内にまで到達することが判明した。続いて，各非晶質シリカを2 mg/headで尾静脈内投与した際の急性毒性を評価した。nSP300やmSP1000を静脈内投与したマウスにおいては急性毒性や肝毒性は全く認められなかったのに対して，nSP70投与マウスは投与後12時間以内に全例が死亡した。また，これらのマウスから回収した血液中の肝障害マーカーを測定したところ，100 nmを閾値に粒子サイズの減少により著しいASTやALTの産生上昇が認められた。これらの結果を重ね合わせると，急性毒性や肝障害性といった生体影響の違いは，非晶質ナノシリカの体内分布特性の差異に起因するものと考えられた。これまで，非晶質ナノシリカが経皮塗布後に体内吸収性や脳内蓄積性を示すといった報告は世界的に見ても皆無である。非晶質ナノシリカが非常に強固な皮膚角質バリアを通過して生体内に移行し，さらに脳をはじめとする各臓器に到達するという事実は非常に興味深く，少なくともこれらの事実は，直径100 nm以下の非晶質ナノシリカがサブミクロンサイズの非晶質シリカとは異なる体内／細胞内動態特性を

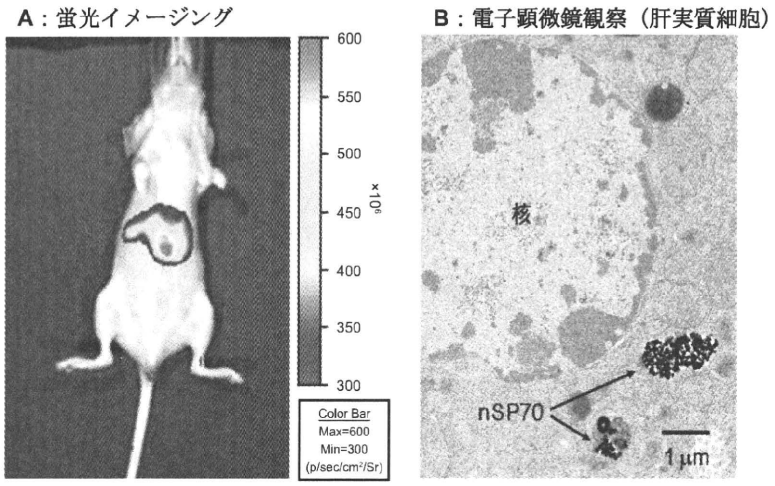

図3　nSP70の体内動態解析。DY676で標識したnSP70（7×10^{10}個）をBALB/cマウス（雌，8週齢）の尾静脈内より投与した。投与24時間後にXenogen IVIS 200を用いてnSP70の局在を蛍光イメージングにより解析した（A）。また，同様にnSP70を投与したマウスから肝臓を回収し，電子顕微鏡を用いてnSP70の肝臓内局在を観察した（B）。

発揮する可能性を示している。現在，我々は，安全性評価において最も重要な経皮吸収量（曝露量）の評価を進めると共に，皮膚透過機構の解析や皮膚局所における安全性評価を推進している。

非晶質ナノシリカの細胞内動態と安全性との連関追求

ここまでの検討結果から，直径100 nm以下の非晶質ナノシリカがサブミクロンサイズの従来素材とは異なる動態特性を発揮し，ナノマテリアルの動態情報を基盤とした安全性評価が重要であることを明らかにした。そこで次に，非晶質ナノシリカの細胞内動態特性と安全性の連関解析を試みた。まず，ヒト皮膚角化細胞株（HaCaT細胞）を用いて，非晶質ナノシリカの細胞内局在を解析した。HaCaT細胞に各粒子サイズの非晶質シリカを添加し，24時間後の細胞をTEMで観察した。その結果，nSP300あるいはmSP1000作用群では，各シリカが細胞内に侵入した像が認められ，特にmSP1000作用群においては細菌感染時と同様のリソソーム小胞の過形成を認めた。それに対して，nSP70は細胞内に侵入するばかりか，核膜を透過して核内に侵入していた。これらの事実は，直径が100 nm以下のナノマテリアルが従来までのマイクロメートルサイズのマテリアルとは異なる細胞内動態特性を示すことを裏付けている。即ち，ナノマテリアルの安全性を確保するに当たっては，細胞内取り込み経路や細胞内オルガネラへの到達性，およびその機構などの細胞内動態に関して精査し，それらの情報を基盤とした安全性評価が必須であると考えられる。特に今回使用した非晶質ナノシリカの場合は，核内移行特性を反映した遺伝子や核機能に対する影響の評価が必要であると考えられた。そこで，コメットアッセイにより，非晶質シリカ処理によるDNA損傷の有無を検討したところ，nSP70作用群においてのみ強力なDNA損傷効果が認められた。これらの結果は，非晶質ナノシリカが粒子径の減少を反映して細胞傷害やDNA損傷を誘発し，発がんリスクを増大させ得ることを示している。今後は，nSP70の核内移行性とDNA損傷との因果関係を精査すると共に，発がん性試験などを検討する必要があると考えられる。

非晶質ナノシリカの起炎性評価および炎症惹起メカニズムの解明

これまでに，生体に取り込まれた粒子状異物排除の根幹を担う免疫担当細胞が，ナノマテリアルを異物として認識した際に，過剰反応や機能不全を起こす可能性が報告されており(6, 13)，ナノマテリアルが未知の免疫撹乱作用を呈する危険性が指摘されている(14)。これらは，ナノマテリアルへの長期・多量曝露が，炎症性疾患や自己免疫疾患，あるいは感染症罹患率の増大など，予期せぬ毒性を引き起こす可能性を示している。我々はこれまでに，サブミクロンサイズの非晶質シリカが，細胞にエンドサイトーシスで取り込まれた後，活性酸素の産生を誘発し，活性酸素がリソソームを破壊することでカテプシンBを細胞質に流出させ，インフラマソームの活性化を誘導することで炎症を惹起することを明らかとしている(15)。しかし，ナノメートルサイズの非晶質ナノシリカの起炎性については，世界的にも明らかとなっていない。さらに上述したように，nSP70のみ経皮吸収性を有し，その後，リンパ節・脾臓のリンパ球や貪食細胞であるマクロファージに多く取り込まれることを明らかとしていることからも，nSP70の免疫機能への影響評価は最優先課題と考えられる。

そこで，粒子径の異なる非晶質シリカの起炎性について，マウスを用いて比較検討した。各粒子径の非晶質シ

リカをマウス腹腔内へと投与し，24時間後における腹腔内の総細胞数を起炎性の指標として評価した。その結果，nSP300，mSP1000投与群では細胞数の増大はほとんど観察されなかったのに対して，nSP70投与群においては，有意な細胞浸潤数の増大が認められるなど，非晶質ナノシリカは強い起炎性を有する可能性が示された。さらに，各非晶質シリカ投与2時間後における腹腔内のサイトカイン産生パターンを解析した結果，nSP70投与群では，炎症性サイトカインやケモカインの産生が認められた。以上の結果より，非晶質シリカは粒子径の減少に従って起炎性が上昇することが明らかとなった。しかし，本結果はあくまでも腹腔内への大量投与による検討であるため，今後，曝露実態を考慮した投与ルートや投与量での検討，更には閾値の解明が必須であると考えられる。

粒子状物質が生体内に取り込まれた場合，まず貪食細胞であるマクロファージに認識されることで免疫応答が誘導される。そこで，代表的なマウスマクロファージ細胞株であるRAW264.7細胞を用いて，非晶質シリカの起炎性をin vitroで評価した。RAW264.7細胞に各非晶質シリカを作用させ，培養上清中に産生される腫瘍壊死因子（TNFα）量をELISAにより評価した。その結果，nSP300，mSP1000作用群におけるTNFαの産生量は未処理群とほぼ同程度であったのに対し，nSP70作用群では有意なTNFαの産生亢進が観察された。本結果より，nSP70はマクロファージからのTNFαなど炎症性サイトカインの産生を誘導することで，炎症を惹起する可能性が示された。

次に，非晶質ナノシリカによるTNFαの産生誘導メカニズムを解析した。細胞が外部からのストレスやサイトカイン刺激を受けると，MAPKファミリーであるp38，c-jun N-terminal kinase（JNK）及びExtracellular Signal-regulated Kinase 1/2（ERK1/2）がリン酸化を受けて活性化し，炎症応答や細胞分化，細胞死など，多様な細胞応答に関わるシグナルを伝達することが知られている。そこで，RAW264.7細胞に各粒子径の非晶質シリカを作用させ，各MAPKの活性化を評価した。その結果，nSP300，mSP1000は，いずれのMAPKも活性化しなかったのに対して，nSP70は全てのMAPKを強く活性化することが明らかとなった。次に，各MAPK阻害剤存在下で，nSP70をRAW264.7細胞に添加し，TNFαの産生量をELISAにより評価した。その結果，nSP70単独で作用させた場合，有意なTNFαの産生上昇が認められたのに対し，いずれのMAPK阻害剤作用条件下においても，nSP70によるTNFαの産生は未処理群と同程度にまで抑制された。本結果は，nSP70がp38，JNK，ERK1/2全ての活性化を介してTNFαの産生を誘導することを示すものである（図4）。

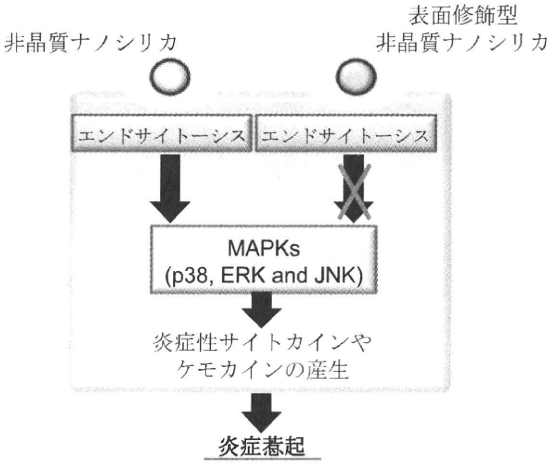

図4　非晶質ナノシリカの起炎性惹起メカニズムの模式図

起炎性の少ない安全なナノマテリアル開発に向けた取り組み

次に，起炎性の少ない非晶質ナノシリカの開発に向けた基礎情報の集積を目的に，非晶質ナノシリカの表面修飾がその起炎性に与える影響を検討した。本検討では，nSP70の表面をカルボキシル基で修飾したnSP70-Cを用いて起炎性を評価した。まず，RAW264.7細胞を用いて，nSP70及びnSP70-CのTNFα産生誘導能を比較した。その結果，nSP70作用群ではTNFαの産生量が増加するのに対し，nSP70-C作用群では全く増加が認められなかった。また，RAW264.7細胞におけるMAPKの活性化を評価した結果，nSP70作用群では，全てのMAPKが活性化されるのに対して，nSP70-C作用群ではいずれのMAPKの活性化も認められなかった。従って，nSP70はカルボキシル基修飾によって，MAPKの活性化が強く抑えられた結果，TNFαの産生が大幅に減弱した可能性が示された。さらに，nSP70及びnSP70-Cをマウス腹腔内に投与し，腹腔内の総細胞数を指標に起炎性を評価した。その結果，nSP70投与群で腹腔内総細胞数が顕著に上昇するのに対し，nSP70-C投与群は細胞数の上昇はほとんど認められず，未処理群との有意な差は観察されなかった。以上の結果より，nSP70の有する起炎性は，表面のカルボキシル基修飾によって抑制可能であることが判明した。

終わりに

現在，ナノマテリアルの生体影響に関する詳細な情報を可能な限り早急に収集する必要性が世界的に叫ばれており，OECDでは，2006年から「工業ナノ材料作業部会」を設置し，安全性に対する論議を精力的に進めている。その一方で，ナノマテリアルは人類のQOL向上に必須の新素材になる可能性を秘めているため，安全性に関するデータが不十分なまま施行された無闇な規制によって，ナノマテリアルの社会受容が阻害され，ひいてはナノマテリアルによって得られるべき恩恵を闇に葬ることだけは避けねばならない。さらに，種々ナノマテリアル配合製品が既に実用化・販売され，ナノマテリアルの人体曝露を避け得ない現状では，危険性のみを闇雲に指摘する